

gene delivery agents [27]. In addition, we found out that the gene delivery was only observed at the site of ultrasound exposure. Therefore, using Bubble liposomes and ultrasound, we could establish minimally-invasive and tumor tissue-specific gene delivery. In the present study, the characteristics of Bubble liposomes as gene delivery vectors were studied, and gene transfection efficiencies into tumor *in vivo* were compared with lipofection using cationic liposomes, a common non-viral gene transfer method.

2. Materials and methods

2.1. Cells

African green monkey kidney fibroblast COS-7 cells were cultured in Dulbecco's modified Eagle's medium (DMEM; Sigma Chemical Co., St. Louis, MO) supplemented with 10% heat inactivated fetal Bovine serum (FBS, GIBCO, Invitrogen Co., Carlsbad, CA). Mouse Sarcoma-180 (S-180) cells were cultured in Eagle's medium (MEM; Sigma) supplemented with 10% heat inactivated FBS. All culture media contained 100 U/mL penicillin (Wako Pure Chemical Industries, Ltd., Osaka, Japan) and 100 µg/mL streptomycin (Wako).

2.2. Preparation of liposomes and Bubble liposomes

Liposomes composed of 1,2-distearoyl-sn-glycero-phosphatidylcholine (DSPC) (NOF Corporation, Tokyo, Japan) and 1,2-distearoyl-sn-glycero-3-phosphatidyl-ethanolamine-methoxy-polyethyleneglycol (DSPE-PEG (2 k)-OME; NOF) (94:6 (m/m)) were prepared by reverse phase evaporation. In brief, all reagents (total lipid: 100 µmol) were dissolved in 8 mL of 1:1 (v/v) chloroform/diisopropyl ether, then 4 mL of PBS was added. The mixture was sonicated and evaporated at 65 °C. The solvent was completely removed, and the size of the liposomes was adjusted to less than 200 nm using an extruding apparatus (Northern Lipids Inc., Vancouver, BC) and sizing filters (pore sizes: 100 nm and 200 nm; Nuclepore Track-Etch Membrane, Whatman plc, UK). After sizing, the liposomes were sterilized by passing them through a 0.45 µm pore size filter (MILLEX HV filter unit, Durapore PVDF membrane, Millipore Corporation, MA). The liposome size was measured with dynamic light scattering (ELS-800, Otsuka Electronics Co., Ltd., Osaka, Japan). The average diameter of these liposomes were about 150–200 nm. Lipid concentration was measured with the Phospholipid C test wako (Wako Pure Chemical Industries). Bubble liposomes were prepared from the liposomes and perfluoropropane gas (Takachiho Chemical Ind. Co. Ltd., Tokyo, Japan). In brief, 5 mL sterilized vials containing 2 mL of the liposome suspension (lipid concentration: 1 mg/mL) were filled with perfluoropropane, capped and then supercharged with 7.5 mL of perfluoropropane. The vial was placed in a bath-type sonicator (42 kHz, 100 W; BRANSONIC 2510J-DTH, Branson Ultrasonics Co., Danbury, CT) under the condition of positive pressure with perfluoropropane in the vial under the condition of positive pressure with perfluoropropane in the vial for 5 min to form the Bubble liposomes.

2.3. Microscopic observation of Optison and Bubble liposomes and size distribution

Optison (NEPA GENE, CO., LTD., Chiba, Japan) or Bubble liposomes were placed on glass slides, covered with a cover slip and observed with a microscope (Leica MICROSYSTEMS, Wetzlar, Germany) using a darklite illuminator (NEPA GENE). The size distribution of Optison and Bubble liposomes was measured by dynamic light scattering (ELS-800).

2.4. Transmission electron microscopy of Bubble liposomes

Bubble liposomes were suspended into sodium alginate solution (0.2% (w/v) in PBS). This suspension was dropped into calcium chloride solution (100 mM) to hold Bubble liposomes within calcium alginate gel. Then, the beads of calcium alginate gel containing Bubble liposomes were prefixed with 2% glutaraldehyde solution in 0.1 M Cacodylate buffer, post-fixed with 2% OsO₄, dehydrated with an ethanol series, and then embedded in Epan812 (polymerized at 60 °C). Ultrathin sections were made with an ultramicrotome at a thickness of 60–80 nm. Ultrathin sections were mounted on 200 mesh copper grids. They were stained with 2% uranyl acetate for 5 min and Pb for 5 min. The samples were observed with JEOL JEM12000EX at 100 kV. The treatment after prefixation was carried out in Hanaichi Ultrastructure Research Institute Co.,Ltd (Aichi, Japan).

2.5. Transfection of plasmid DNA into cells using Bubble liposomes

Luciferase coding plasmid DNA (pCMV-Luc), COS-7 cells (1×10^5 cells) and Bubble liposomes (60 µg) were suspended in culture medium (500 µL) with 10% FBS in 2 mL polypropylene tubes. The suspension was ultrasonicated using a Sonopore 4000 (6 mm diameter probe; NEPA GENE) sonicator under various conditions. The cells were washed twice with PBS, resuspended in fresh culture medium and cultured in 48-well plates for 2 days.

2.6. Transfection of plasmid DNA into cells by lipofection

Plasmid DNA (pCMV-Luc, 0.25 µg) and Lipofectin (1.25 µg) (Invitrogen) were mixed and complexed according to the manufacturer's instructions. The complex was added to COS-7 cell suspensions (1×10^5 cells/500 µL/tube) containing various concentrations of serum for 10 s. The cells were washed twice with PBS, resuspended in fresh culture medium and cultured in 48-well plates for 2 days.

2.7. *In vivo* gene delivery into mouse ascites tumor cells

S-180 cells (1×10^6 cells) were *i.p.* injected into ddY mice (4 weeks old, male) (Sankyo Labo Service Corporation, Tokyo, Japan) on day 0. When S-180 cells grew as the ascites tumor in mice after 8 days of the injection [28], the mice were anaesthetized with NEMBUTAL (50 mg/kg) (Dainippon

Sumitomo Pharma, Osaka, Japan), then injected with 510 μ L of pCMV-Luc (10 μ g) and Bubble liposomes (500 μ g) in PBS. Ultrasound (frequency: 1 MHz, duty: 50%; intensity: 1.0 W/cm², time: 1 min) was transdermally applied to the abdominal area using a Sonopore 3000 ultrasonicator with a probe of diameter 20mm (NEPA GENE). In other experiments, pCMV-Luc (10 μ g) and Lipofectin (50 μ g) or Lipofectamine 2000 (50 μ g) were mixed and complexed according to the manufacturer's instructions. The complex was suspended in PBS (510 μ L) and injected into the peritoneal cavities of mice. After 2 days, S-180 cells were recovered from the abdomens of the mice. Then, the recovered cells were lysed in the lysis buffer (0.1M Tris-HCl (pH 7.8), 0.1% Triton X-100, 2mM EDTA) and luciferase activity was determined.

2.8. *In vivo* gene delivery into mouse footpad solid tumor

S-180 cells (1×10^6 cells) were inoculated into the left footpad of ddY mice (5 weeks old, male). At day 4, when the thickness of the footpad was over 3.5 mm (normal thickness was about 2 mm), the left femoral artery was exposed. One hundred μ L of pCMV-Luc (10 μ g) with or without Bubble liposomes (100 μ g) were injected into femoral artery using 30-gauge needle. In the same time, ultrasound (frequency: 0.7 MHz, duty: 50%; intensity: 1.2 W/cm², time: 2 min) was transdermally applied to the tumor tissue using a Sonopore 4000 ultrasonicator with a probe of diameter 8 mm (NEPAGENE). The needle hole was then closed with an adhesive agent (Aron Alpha; Sankyo, Tokyo, Japan) and skin was put in a suture. In other samples, pCMV-Luc (10 μ g) and Lipofectamine 2000 (25 μ g) (Invitrogen Corporation, Carlsbad, CA) were mixed and complexed according to manual of Lipofectamine 2000. The complex were suspended in PBS (100 μ L) and injected into femoral artery of mice. After 2 days of injection, the mice were sacrificed and the tumor tissues were collected. Then, the tumor tissues were homogenated in the lysis buffer and luciferase activity was determined.

2.9. Luciferase assay

Luciferase activity was measured using a luciferase assay system (Promega, Madison, WI) and a luminometer (TD-20/20; Turner Designs, Sunnyvale, CA). Activity is reported in relative light units (RLU) per mg protein.

2.10. *In vivo* Luciferase imaging

The mice were anaesthetized and *i.p.* injected with D-luciferin (150 mg/kg) (Xenogen, Corporation, CA). After 10 min, luciferase expression was observed with *in vivo* luciferase imaging system (IVIS) (Xenogen Corporation).

2.11. Hemolysis assay

Mouse red blood cells (2.5×10^8 cells/500 μ L) were exposed with ultrasound (frequency: 0.7 MHz, Duty: 50%, Intensity: 0.5–1.5 W/cm², Time: 10 s.) in absent or present of Bubble

liposomes. The red blood cell suspension was centrifuged for 10 min at 3000 rpm. Then, absorbance ($A_{540 \text{ nm}}$) of the supernatant was measured. The rate of hemolysis was calculated as follows: % of hemolysis = ($A_{540 \text{ nm}}$ of experimental group - $A_{540 \text{ nm}}$ of non-treated group) / ($A_{540 \text{ nm}}$ of hypotonic solution treated group - $A_{540 \text{ nm}}$ of non-treated group) $\times 100$.

2.12. *In vivo* studies

All experimental protocols for animal studies were in accordance with the Principle of Laboratory Animal Care in Teikyo University.

2.13. Statistical analysis

Differences in luciferase activity between experimental groups were compared with non-repeated measures ANOVA and Dunnett's test.

3. Results and discussion

The use of non-viral vectors is attractive as a safe, clinically acceptable gene therapy technique. In addition, non-viral vectors should be easy to prepare and use. However, most non-viral vectors deliver plasmid DNA into cells via endocytosis, followed by plasmid DNA degradation in the endosomes. Consequently, non-viral vectors often result in low gene delivery efficiency. It has been reported that new types of non-viral vectors can induce the escape of genes from endosomes [29–31] and directly deliver genes into the cytosol via a fusion mechanism [28,32]. In addition, microbubbles and ultrasound have been investigated with a view to improving the transfection efficiency of non-viral vectors. Gene delivery using a combination of microbubbles such as Optison and ultrasound has been widely reported. In order for extracellular plasmid DNA to be directly and effectively delivered into the cytosol, transient pores in the cell membrane must be formed by cavitation. However, conventional microbubbles are very large, with most greater than 2 μ m in diameter [16]. Actually, our observations of Optison using a microscope and a darkfield illuminator showed some bubbles more than 10 μ m in diameter (Fig. 1(a)). In the measurement of the size distribution, there were some large microbubbles (Fig. 1d)). Tsunoda et al. pointed out that these large bubbles might cause lethal embolism in some vital organs [17]. In contrast, most Bubble liposomes were much smaller than Optison, with average diameters less than 2 μ m (Fig. 1(b, e)). The injection of 1 mg of Bubble liposomes into the tail veins of mice was not lethal (data not shown), suggesting that Bubble liposomes may not cause lethal embolism. To confirm the structure of Bubble liposomes, we observed Bubble liposome with transmission electron microscopy (Fig. 1(c)). Interestingly, there were nanobubbles into lipid bilayer. From this result, it was thought that Bubble liposomes were different from conventional microbubbles which was the echo gas wrapped with lipid mono-layer. Kodama T. et al. and Klibanov A.L. et al. reported about microbubbles using distearoylphosphatidylcholine and PEG-

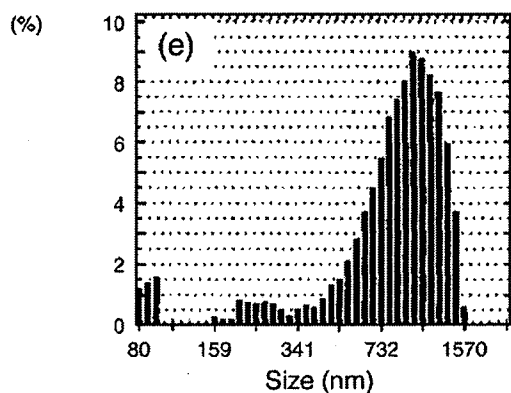
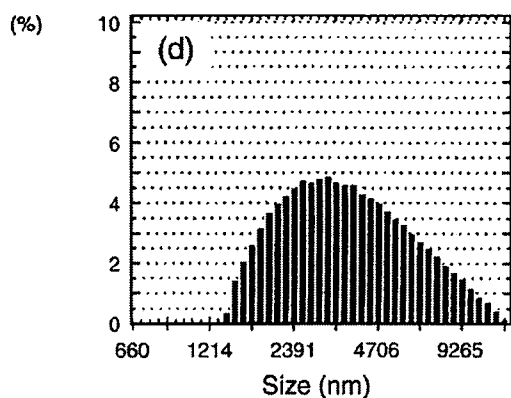
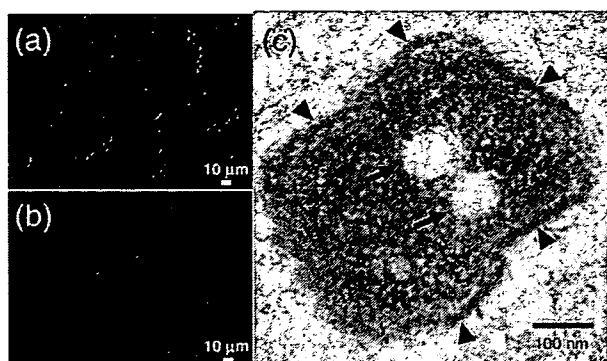


Fig. 1. Microscopy of Optison and Bubble liposomes. Optison (a) and Bubble liposomes (b) were observed with a microscope using a darklite illuminator. Original magnification $\times 400$. Bubble liposomes (c) were observed with a transmission electric microscope at 100 kV. Original magnification $\times 50,000$. Arrow head shows lipid bi-layer and arrow shows perfluoropropane nanobubble. The size distribution of Optison (d) and Bubble liposomes (e).

stearate [33,34]. These microbubbles were made by being stabilized hydrophobic echo gas with amphipathic molecules such as lipid and surfactant. In our method, it was thought that liposomes were reconstituted by sonication under the condition of supercharge with perfluoropropane in the 5 mL vial container. At the same time, perfluoropropane would be entrapped within lipids like micelles, which were made by DSPC and DSPE-PEG (2 k)-OME from liposome composition, to form nanobubbles. The lipid nanobubbles were encapsulated within the reconstituted liposomes (Fig. 1(c)), which sizes were changed into around 1 μm (Fig. 1(b,e)) from 150–200 nm of

original. In addition, we evaluated about the stability of Bubble liposomes by transfection efficiency with sonoporation (Fig. 2). The efficiency gradually decreased according to storage time. We also observed the aspect and ultrasound imaging of Bubble liposomes. The suspension of Bubble liposomes gradually became clear in aspects, resulted in decreasing the echo signal according to storage time (data not shown). These results suggested that perfluoropropane was gradually degassed from Bubble liposomes. Therefore, we used fresh Bubble liposomes in all experiments.

Previously, we reported that Bubble liposomes could induce cavitation and deliver plasmid DNA into various types of cells [27]. In order to examine what conditions are necessary for Bubble liposomes to efficiently deliver genes, transfection efficiency was assessed using Bubble liposomes combined with various levels of ultrasound exposure (Fig. 3(a)). COS-7 cells were exposed to various intensities of ultrasound in the presence of Bubble liposomes for 10 s. Gene transfection efficiency increased with increasing ultrasound intensity and reached a plateau at 0.7 W/cm². No cytotoxicity was evident even at 2.5 W/cm² (data not shown). The length of ultrasound exposure required to achieve gene expression was examined by measuring gene expression after 0, 1, 5 and 10 s of exposure (Fig. 3(b)). Surprisingly, gene expression was observed after 1 s of ultrasound exposure in the presence of Bubble liposomes. Transfection efficiency depended on ultrasound exposure time and reached a plateau after 5 s exposure. Efficiency was found to depend on both ultrasound intensity and exposure time (Fig. 3), indicating that Bubble liposomes can rapidly induce gene delivery while requiring only weak ultrasound, and without inducing cytotoxicity. Five seconds or 0.7 W/cm² of ultrasound exposure resulted in maximal gene expression, presumably due to bubble cavitation.

The transfection efficiency of some cationic non-viral vectors is significantly decreased in the presence of serum

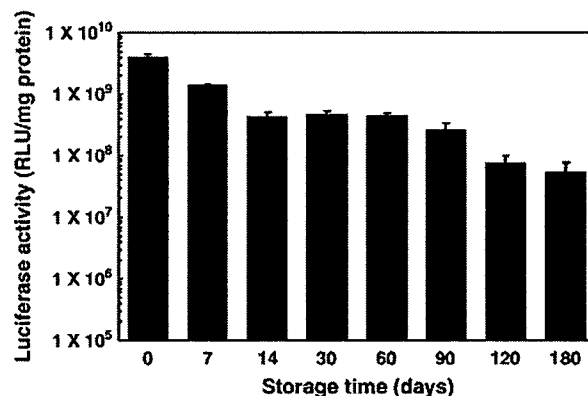


Fig. 2. Stability of Bubble liposomes. After preparation of Bubble liposomes, the vial containing Bubble liposomes was put in the refrigerator for each period. After storage, the transfection efficiency was measured with each samples. COS-7 cells (1×10^5 cells/500 μL) were mixed with pCMV-Luc (5 μg) and Bubble liposomes (60 μg). The cell mixture was exposed to ultrasound (frequency: 2 MHz, duty: 50%, burst rate: 2 Hz, intensity: 2.5 W/cm², time: 10 s). The cells were washed and cultured for 2 days, then luciferase activity was determined as described in Materials and methods. Each bar represents the mean \pm S.D. for triplicate.

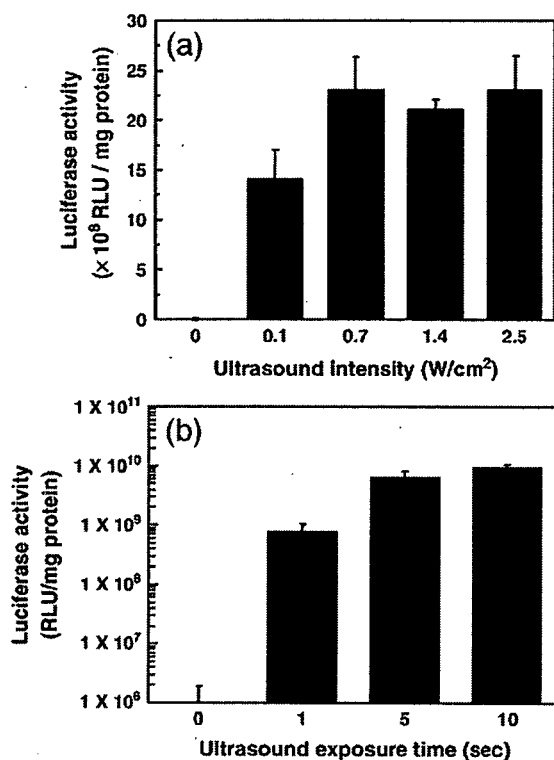


Fig. 3. Effect of ultrasound conditions on transfection efficiency with Bubble liposomes. COS-7 cells (1×10^5 cells/500 μ L) were mixed with pCMV-Luc (5 μ g) and Bubble liposomes (60 μ g). The cell mixture was exposed to ultrasound (a): (frequency: 2 MHz, duty: 50%, burst rate: 2 Hz, intensity: 0–2.5 W/cm^2 , time: 10 s.) or (b): (frequency: 2 MHz, duty: 50%, burst rate: 2 Hz, intensity: 2.5 W/cm^2 , time: 0–10 s.). The cells were washed and cultured for 2 days, then luciferase activity was determined as described in Materials and methods. Each bar represents the mean \pm S.D. for triplicate.

due to an interaction between serum proteins and the cationic vectors [28]. Whereas, transfection efficiency with the combination of Bubble liposomes and ultrasound did not decrease even in the presence of 50% serum in *in vitro* study [27]. In the next examination, we examined whether Bubble liposomes could deliver plasmid DNA into S-180 ascites tumor cells in living animals after local injection (Fig. 4). In this examination, we compared the transfection efficiency with Bubble liposomes or cationic liposomes such as Lipofectin and Lipofectamine 2000. Luciferase expression was low in the mice treated with lipofectin-plasmid DNA complexes prepared by the traditional lipofection method, presumably because the complexes were associated with various proteins in the peritoneal cavity. On the other hand, luciferase expression increased in the mice treated with Lipofectamine 2000-plasmid DNA complexes compare with Lipofectin, because it was known that LF2000 was better than Lipofectin for gene delivery in the presence of serum. In addition, luciferase expression in mice treated with plasmid DNA, Bubble liposomes and ultrasound exposure was higher than that in the mice treated with Lipofectamine 2000-plasmid DNA complexes. This result supported the previous our report. In short, it was thought that Bubble liposomes and ultrasound was not affected by proteins existing in the peritoneal cavity and this method immediately and directly delivered plasmid DNA

into cells with the mechanism which was not endocytosis pathway in lipofection method. We also confirmed that ultrasound combined with Bubble liposomes was effective at delivering genes to other tissues in the peritoneal cavity such as stomach, kidney, liver, spleen, intestine, diaphragm, pancreas, peritoneum and mesentery. Luciferase activity in these tissues was much lower than that observed in the S-180 cells (less than 130 RLU/mg protein).

Mizuguchi et al. reported about the effective cancer gene therapy by cytokine provision in the local area via gene delivery into arteries leading to tumor or arteries in tumor tissue [35]. Previously, we succeeded the gene delivery into artery of ultrasound exposure site with Bubble liposomes [27]. Therefore, we thought that our technology could be applied to establish the tumor tissue specific gene delivery. In this time, we attempted to deliver plasmid DNA to solid tumor via the injection into the artery that lead to tumor (Fig. 5). In Fig. 4, Lipofectin did not work well as gene delivery tool. In this study, we only used Lipofectamine 2000 as a control. In the mice treated with plasmid DNA and ultrasound, luciferase expression was same low level in the mice of plasmid DNA injection. And, luciferase expression was also low level in the mice treated with Lipofectamine 2000 and plasmid DNA complex, although the complex could be induced into S-180 ascites tumor cells. Generally, enough time is necessary for the complex to bind to cell surface and deliver plasmid DNA into cells. In this case, there was no time for the complex to retain in tumor tissue after injection because of blood stream and it would be resulted in

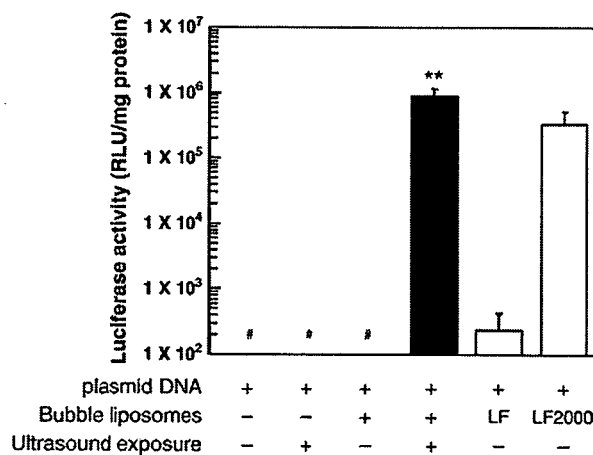


Fig. 4. *In vivo* gene delivery into mouse ascites tumor cells with Bubble liposomes. S-180 cells (1×10^6 cells) were i.p. injected into ddY mice. After 8 days, the mice were anaesthetized, then injected with 510 μ L of pCMV-Luc (10 μ g) and Bubble liposomes (500 μ g) in PBS. Ultrasound (frequency: 1 MHz, duty: 50%; intensity: 1.0 W/cm^2 , time: 1 min) was transdermally applied to the abdominal area. In another experiment, pCMV-Luc (10 μ g) — Lipofectin (50 μ g) or Lipofectamine 2000 (50 μ g) complex was suspended in PBS (510 μ L) and injected into the peritoneal cavity of mice. After 2 days, S-180 cells were recovered from the abdomens of the mice. Luciferase activity was determined as described in Materials and methods. Each bar represents the mean \pm S.D. for three to six mice/group. ** $P < 0.01$ compared to the group treated with plasmid DNA, Bubble liposomes, ultrasound exposure or lipofection with Lipofectin or Lipofectamine 2000. LF, Lipofectin. LF2000, Lipofectamine 2000. # $< 10^2$ RLU/mg protein.

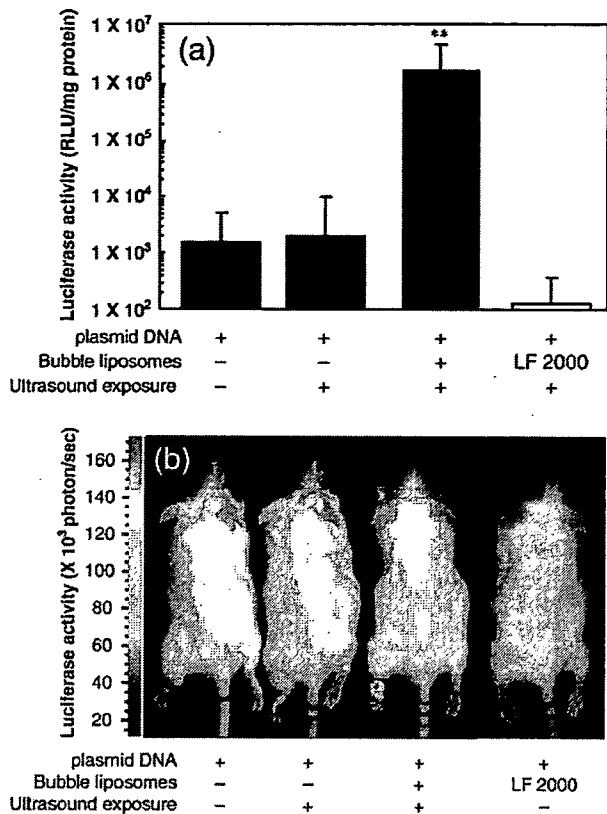


Fig. 5. *In vivo* gene delivery into mouse solid tumor with Bubble liposomes. S-180 cells (1×10^6 cells) were inoculated into left footpad of ddY mice. After 4 days, the mice were anaesthetized, then injected with 100 μ L of pCMV-Luc (10 μ g) in absent or present of Bubble liposomes (100 μ g) in PBS. Ultrasound (frequency: 0.7 MHz, duty: 50%; intensity: 1.2 W/cm², time: 1 min) was transdermally exposed to tumor tissue. In another experiment, pCMV-Luc (10 μ g) — Lipofectamine 2000 (25 μ g) complex was suspended in PBS (100 μ L) and injected into the left femoral artery. After 2 days, tumor tissue was recovered the mice. Luciferase activity was determined as described in Materials and methods. (a) Luciferase activity in solid tumor. Each bar represents the mean \pm S.D. for five mice/group. ** $P < 0.01$ compared to the group treated with plasmid DNA, ultrasound exposure or Lipofectamine 2000. (b) *In vivo* luciferase imaging in the solid tumor bearing mice. The photon counts are indicated by the pseudo-color scales. LF 2000, Lipofectamine 2000.

low efficiency of transfection. On the other hand, luciferase expression in the combination of Bubble liposomes and ultrasound was much higher than that in other group (Fig. 5(a)). Koch et al. reported that the combination of ultrasound and microbubble (Levovist) enhanced lipoplex-mediated cell transfection efficiency *in vitro* and also severely damaged most cells. [36]. Therefore, we attempted to confirm the enhancement of transfection efficiency with Lipofectamine 2000 by Bubble liposomes and ultrasound in the condition without cell damage. The transfection efficiency with lipoplex was not enhanced with Bubble liposomes and ultrasound *in vitro* and *in vivo* (data not shown). The size of Lipofectamine 2000-plasmid DNA complexes was larger than that of naked plasmid DNA by forming the spaghetti–meatball like structure. We guessed that it was difficult for the complexes to enter into cytosol via transient pore on the membrane with cavitation of Bubble liposomes in the condition without cell damage. In the Koch's

report, ultrasound was exposed to *in vitro* cells for 60 s with Levovist (20 and 200 mg/mL). In this study, Bubble liposomes (1 mg/mL) were injected into the femoral artery. The concentration of Bubble liposomes would be much lower than that of Levovist because of the dilution of Bubble liposomes in the blood. In addition, the time of ultrasound exposure to Bubble liposomes was very short because of blood flow. Therefore, I thought that the transfection efficiency in the combination of cavitation with Bubble liposomes and lipoplexes was not enhanced. To evaluate gene expression site, we observed luciferase expression with luciferase *in vivo* imaging system (Fig. 5(b)). In the mice treated with Bubble liposomes and ultrasound, luciferase expression was observed in the tumor tissue because of inducing cavitation at ultrasound exposure site. Then, there were a possibility of hemolysis by the cavitation of Bubble liposomes in artery. We examined about hemolytic effect in the treatment of Bubble liposomes and ultrasound (Fig. 6). When the ultrasound was exposed to red blood cell with or without Bubble liposomes *in vitro*, serious hemolysis was not induced. These results suggested that this gene delivery system was important method to achieve tumor specific gene delivery without serious damage.

Plasmid DNA was effectively delivered into S-180 ascites tumor cells and solid tumor tissues with Bubble liposomes and ultrasound, although plasmid DNA did not form a complex with Bubble liposomes because Bubble liposomes were made of neutral charge lipids and modified polyethylene glycol on the surface, and existed free *in vivo*. These results could be explained from Fig. 3. In short, it is thought that Bubble liposomes can immediately and effectively deliver plasmid DNA into cells *in vivo* before the plasmid DNA is degraded by DNase. A mixture of plasmid DNA and Bubble liposomes was injected into mice, and the plasmid DNA was delivered to a specific area of the abdomen or solid tumor tissue by local exposure to ultrasound, suggesting that gene targeting can be induced at a site by exposure to ultrasound. In future studies, we intend to establish minimally-invasive and tissue-specific gene delivery with Bubble liposomes after systemic injection.

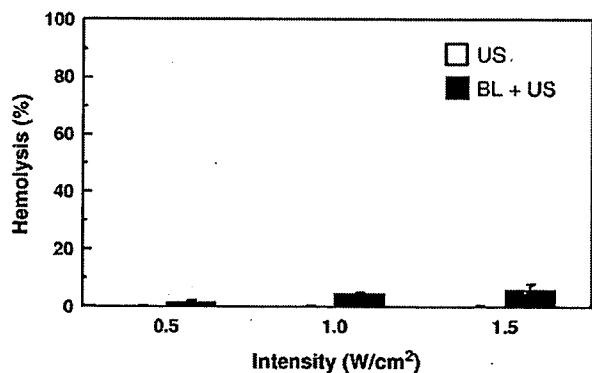


Fig. 6. Hemolysis of red blood cells by Bubble liposomes and ultrasound. Mouse red blood cells (2.5×10^8 cells/ 500 mL) were exposed with ultrasound (frequency: 0.7 MHz, Duty: 50%, Intensity: 0.5–1.5 W/cm², Time: 10 s) in absent or present of Bubble liposomes. Hemolysis was assessed as described in Materials and methods. Each bar represents the mean \pm S.D. for triplicate.

The present study showed that Bubble liposomes can be a more effective gene delivery tools into tumor *in vivo* than conventional lipofection. Moreover, Bubble liposomes are an attractive gene delivery approach in cancer gene therapy as the method is minimally-invasive and tumor specific gene transfer, requiring only exposure to ultrasound applied to the surface of the body.

Acknowledgements

We are grateful to Dr. Katsuro Tachibana (Department of Anatomy, School of Medicine, Fukuoka University) for technical advice regarding the induction of cavitation with ultrasound, to Mr. Katsutoshi Kurosawa, Mr. Takamichi Todoroki, Ms. Hitomi Tamagawa (Department of Biopharmaceutics, School of Pharmaceutical Sciences, Teikyo University) for excellent technical assistance, to Dr. Akinori Suginaka (NOF CORPORATION) for technical advice regarding lipids and for providing the lipids, and to Mr. Yasuhiko Hayakawa, Mr. Takahiro Yamauchi and Mr. Kosho Suzuki (NEPA GENE CO., LTD.) for technical advice regarding ultrasound exposure.

This study was supported by an Industrial Technology Research Grant (04A05010) in 2004 from the New Energy and Industrial Technology Development Organization (NEDO) of Japan, a Grant-in-Aid for Young Scientists (160700392, 19700423), Exploratory Research (16650126) from the Japan Society for the Promotion of Science and a Research on Advanced Medical Technology (17070301) in Health and Labour Sciences Research Grants from Ministry of Health, Labour and Welfare.

References

- [1] M. Fechheimer, J.F. Boylan, S. Parker, J.E. Siskin, G.L. Patel, S.G. Zimmer, Transfection of mammalian cells with plasmid DNA by scrape loading and sonication loading, *Proc. Natl. Acad. Sci. U. S. A.* 84 (1987) 8463–8467.
- [2] M.W. Miller, D.L. Miller, A.A. Brayman, A review of *in vitro* bioeffects of inertial ultrasonic cavitation from a mechanistic perspective, *Ultrasound Med. Biol.* 22 (1996) 1131–1154.
- [3] M. Joersbo, J. Brunstedt, Protein synthesis stimulated in sonicated sugar beet cells and protoplasts, *Ultrasound Med. Biol.* 16 (1990) 719–724.
- [4] H.R. Guzman, A.J. McNamara, D.X. Nguyen, M.R. Prausnitz, Bioeffects caused by changes in acoustic cavitation bubble density and cell concentration: a unified explanation based on cell-to-bubble ratio and blast radius, *Ultrasound Med. Biol.* 29 (2003) 1211–1222.
- [5] D.L. Miller, S.V. Pislaru, J.E. Greenleaf, Sonoporation: mechanical DNA delivery by ultrasonic cavitation, *Somat. Cell Mol. Genet.* 27 (2002) 115–134.
- [6] W. Wei, B. Zheng-zhong, W. Yong-jie, Z. Qing-wu, M. Ya-lin, Bioeffects of low-frequency ultrasonic gene delivery and safety on cell membrane permeability control, *J. Ultrasound. Med.* 23 (2004) 1569–1582.
- [7] M. Duvshani-Eshet, M. Machluf, Therapeutic ultrasound optimization for gene delivery: a key factor achieving nuclear DNA localization, *J. Control Release* 108 (2005) 513–528.
- [8] H.J. Kim, J.F. Greenleaf, R.R. Kinnick, J.T. Bronk, M.E. Bolander, Ultrasound-mediated transfection of mammalian cells, *Hum. Gene Ther.* 7 (1996) 1339–1346.
- [9] D.B. Tata, F. Dunn, D.J. Tindall, Selective clinical ultrasound signals mediate differential gene transfer and expression in two human prostate cancer cell lines: LnCap and PC-3, *Biochem. Biophys. Res. Commun.* 234 (1997) 64–67.
- [10] W.J. Greenleaf, M.E. Bolander, G. Sarkar, M.B. Goldring, J.F. Greenleaf, Artificial cavitation nuclei significantly enhance acoustically induced cell transfection, *Ultrasound Med. Biol.* 24 (1998) 587–595.
- [11] T. Li, K. Tachibana, M. Kuroki, M. Kuroki, Gene transfer with echo-enhanced contrast agents: comparison between Albunex, Optison, and Levovist in mice-initial results, *Radiology* 229 (2003) 423–428.
- [12] R.V. Shohet, S. Chen, Y.T. Zhou, Z. Wang, R.S. Meidell, R.H. Unger, P.A. Grayburn, Echocardiographic destruction of albumin microbubbles directs gene delivery to the myocardium, *Circulation* 101 (2000) 2554–2556.
- [13] S. Sonoda, K. Tachibana, E. Uchino, A. Okubo, M. Yamamoto, K. Sakoda, T. Hisatomi, K.H. Sonoda, Y. Negishi, Y. Izumi, S. Takao, T. Sakamoto, Gene transfer to corneal epithelium and keratocytes mediated by ultrasound with microbubbles, *Investig. Ophthalmol. Vis. Sci.* 47 (2006) 558–564.
- [14] Y. Taniyama, K. Tachibana, K. Hiraoka, M. Aoki, S. Yamamoto, K. Matsumoto, T. Nakamura, T. Ogihara, Y. Kaneda, R. Morishita, Development of safe and efficient novel nonviral gene transfer using ultrasound: enhancement of transfection efficiency of naked plasmid DNA in skeletal muscle, *Gene Ther.* 9 (2002) 372–380.
- [15] Y. Taniyama, K. Tachibana, K. Hiraoka, T. Namba, K. Yamasaki, N. Hashiya, M. Aoki, T. Ogihara, K. Yasufumi, R. Morishita, Local delivery of plasmid DNA into rat carotid artery using ultrasound, *Circulation* 105 (2002) 1233–1239.
- [16] J.R. Lindner, Microbubbles in medical imaging: current applications and future directions, *Nat. Rev. Drug Discov.* 3 (2004) 527–532.
- [17] S. Tsunoda, O. Mazda, Y. Oda, Y. Iida, S. Akabame, T. Kishida, M. Shin-Ya, H. Asada, S. Gojo, J. Imanishi, H. Matsubara, T. Yoshikawa, Sonoporation using microbubble BR14 promotes pDNA/siRNA transduction to murine heart, *Biochem. Biophys. Res. Commun.* 336 (2005) 118–127.
- [18] M. Harata, Y. Soda, K. Tani, J. Ooi, T. Takizawa, M. Chen, Y. Bai, K. Izawa, S. Kobayashi, A. Tomonari, F. Nagamura, S. Takahashi, K. Uchimar, T. Iseki, T. Tsuji, T.A. Takahashi, K. Sugita, S. Nakazawa, A. Tojo, K. Maruyama, S. Asano, CD19-targeting liposomes containing imatinib efficiently kill Philadelphia chromosome-positive acute lymphoblastic leukemia cells, *Blood* 104 (2004) 1442–1449.
- [19] O. Ishida, K. Maruyama, H. Tanahashi, M. Iwatsuru, K. Sasaki, M. Eriguchi, H. Yanagie, Liposomes bearing polyethyleneglycol-coupled transferrin with intracellular targeting property to the solid tumors *in vivo*, *Pharm. Res.* 18 (2001) 1042–1048.
- [20] K. Kawamura, N. Kadowaki, R. Suzuki, S. Udagawa, S. Kasaoka, N. Utoguchi, T. Kitawaki, N. Sugimoto, N. Okada, K. Maruyama, T. Uchiyama, Dendritic cells that endocytosed antigen-containing IgG-liposomes elicit effective antitumor immunity, *J. Immunother.* 29 (2006) 165–174.
- [21] K. Maruyama, E. Holmberg, S.J. Kennel, A. Klibanov, V.P. Torchilin, L. Huang, Characterization of *in vivo* immunoliposome targeting to pulmonary endothelium, *J. Pharm. Sci.* 79 (1990) 978–984.
- [22] K. Maruyama, O. Ishida, S. Kasaoka, M. Eriguchi, H. Yanagie, Intracellular targeting of sodium mercaptoundecahydrodecaborate (BSH) to solid tumors by transferrin-PEG liposomes, for boron neutron-capture therapy (BNCT), *J. Control. Release* 98 (2004) 195–207.
- [23] K. Maruyama, S.J. Kennel, L. Huang, Lipid composition is important for highly efficient target binding and retention of immunoliposomes, *Proc. Natl. Acad. Sci. U. S. A.* 87 (1990) 5744–5748.
- [24] H. Yanagie, K. Maruyama, T. Takizawa, O. Ishida, K. Ogura, T. Matsumoto, Y. Sakurai, T. Kobayashi, A. Shinohara, J. Rant, J. Skvarc, R. Illic, G. Kuhne, M. Chiba, Y. Furuya, H. Sugiyama, T. Hisa, K. Ono, H. Kobayashi, M. Eriguchi, Application of boron-entrapped stealth liposomes to inhibition of growth of tumour cells in the *in vivo* boron neutron-capture therapy model, *Biomed. Pharmacother.* 60 (2006) 43–50.
- [25] H. Yanagie, K. Ogura, K. Takagi, K. Maruyama, T. Matsumoto, Y. Sakurai, J. Skvarc, R. Illic, G. Kuhne, T. Hisa, I. Yoshizaki, K. Kono, Y. Furuya, H. Sugiyama, H. Kobayashi, K. Ono, K. Nakagawa, M. Eriguchi, Accumulation of boron compounds to tumor with polyethylene-glycol binding liposome by using neutron capture autoradiography, *Appl. Radiat. Isotopes* 61 (2004) 639–646.
- [26] H. Hatakeyama, H. Akita, K. Kogure, M. Oishi, Y. Nagasaki, Y. Kihira, M. Ueno, H. Kobayashi, H. Kikuchi, H. Harashima, Development of a novel

- systemic gene delivery system for cancer therapy with a tumor-specific cleavable PEG-lipid, *Gene Ther.* 14 (2007) 68–77.
- [27] R. Suzuki, T. Takizawa, Y. Negishi, K. Hagiwara, K. Tanaka, K. Sawamura, N. Utoguchi, T. Nishioka, K. Maruyama, Gene delivery by combination of novel liposomal bubbles with perfluoropropane and ultrasound, *J. Control. Release* 117 (2007) 130–136.
- [28] H. Mizuguchi, T. Nakagawa, M. Nakanishi, S. Imazu, S. Nakagawa, T. Mayumi, Efficient gene transfer into mammalian cells using fusogenic liposome, *Biochem. Biophys. Res. Commun.* 218 (1996) 402–407.
- [29] K. Kono, Y. Torikoshi, M. Mitsutomi, T. Itoh, N. Emi, H. Yanagie, T. Takagishi, Novel gene delivery systems: complexes of fusogenic polymer-modified liposomes and lipoplexes, *Gene Ther.* 8 (2001) 5–12.
- [30] N. Sakaguchi, C. Kojima, A. Harada, K. Koiwai, K. Shimizu, N. Emi, K. Kono, Enhancement of transfection activity of lipoplexes by complexation with transferrin-bearing fusogenic polymer-modified liposomes, *Int. J. Pharm.* 325 (2006) 186–190.
- [31] T. Kakudo, S. Chaki, S. Futaki, I. Nakase, K. Akaji, T. Kawakami, K. Maruyama, H. Kamiya, H. Harashima, Transferrin-modified liposomes equipped with a pH-sensitive fusogenic peptide: an artificial viral-like delivery system, *Biochemistry* 43 (2004) 5618–5628.
- [32] M. Kondoh, T. Matsuyama, R. Suzuki, H. Mizuguchi, T. Nakanishi, S. Nakagawa, Y. Tsutsumi, M. Nakanishi, M. Sato, T. Mayumi, Growth inhibition of human leukemia HL-60 cells by an antisense phosphodiester oligonucleotide encapsulated into fusogenic liposomes, *Biol. Pharm. Bull.* 23 (2000) 1011–1013.
- [33] H. Leong-Poi, J. Christiansen, A.L. Klibanov, S. Kaul, J.R. Lindner, Noninvasive assessment of angiogenesis by ultrasound and microbubbles targeted to $\alpha(v)$ -integrins, *Circulation* 107 (2003) 455–460.
- [34] M. Takahashi, K. Kido, A. Aoi, H. Furukawa, M. Ono, T. Kodama, Spinal gene transfer using ultrasound and microbubbles, *J. Control. Release* 117 (2007) 267–272.
- [35] H. Mizuguchi, T. Nakagawa, S. Toyosawa, M. Nakanishi, S. Imazu, T. Nakanishi, Y. Tsutsumi, S. Nakagawa, T. Hayakawa, N. Ijuhin, T. Mayumi, Tumor necrosis factor α -mediated tumor regression by the in vivo transfer of genes into the artery that leads to tumors, *Cancer Res.* 58 (1998) 5725–5730.
- [36] S. Koch, P. Pohl, U. Cobet, N.G. Rainov, Ultrasound enhancement of liposome-mediated cell transfection is caused by cavitation effects, *Ultrasound Med. Biol.* 26 (2000) 897–903.

Effective gene delivery with liposomal bubbles and ultrasound as novel non-viral system

RYO SUZUKI¹, TOMOKO TAKIZAWA¹, YOICHI NEGISHI², NAOKI UTOGUCHI¹, & KAZUO MARUYAMA¹

¹Department of Pharmaceutical Sciences, School of Pharmaceutical Sciences, Teikyo University, Sagami-hara, Kanagawa, Japan, and ²Department of Drug and Gene Delivery System, School of Pharmacy, Tokyo University of Pharmacy and Life Sciences, Hachioji, Tokyo, Japan

(Received 8 June 2007; accepted 8 June 2007)

Abstract

We developed the novel liposomal bubbles (Bubble liposomes) containing ultrasound imaging gas, perfluoropropane. Bubble liposomes were made of pegylated liposomes and were smaller than conventional microbubbles. Bubble liposomes also had a function as imaging agents in cardiosonography. In addition, Bubble liposomes could deliver plasmid DNA into various types of cells *in vitro* without cytotoxicity by the combination of ultrasound. *In vivo* gene delivery, Bubble liposomes could deliver plasmid DNA into mouse femoral artery by the transdermal exposure of ultrasound. This transfection efficiency was more effectively than lipofection method. Interestingly, the gene expression was only observed at the site of ultrasound exposure. Therefore, we concluded that Bubble liposomes could be good tools to establish tissue-specific gene delivery system as well as ultrasound imaging agents.

Keywords: Liposome, ultrasound, gene delivery, cavitation, sonoporation, perfluoropropane

Introduction

Gene therapy has potential in the treatment of cancer and diseases that are due to genomic causes. In addition, at present gene therapy is applied into cardiovascular diseases. Especially, in arteriosclerosis obliterans (ASO), vascular endothelial growth factor and hepatocyte growth factor (HGF) gene therapies have been reported to have beneficial effects. Although viral vector systems are efficient gene delivery tools, some problems have been reported (Marshall 1999; Check 2002, 2003). In this situation, non-viral gene delivery systems became to be paid attention (Conwell and Huang 2005). However, their transduction efficiency is very low. Efforts have recently been directed towards improving this aspect (Mizuguchi et al. 1996; Kogure et al. 2004; Wada et al. 2005).

In 1987, Fechheimer et al. (1987) reported a new concept about application of ultrasound energy for gene delivery. And ultrasound has gained wide interest in gene therapy due to its potential to deliver genes into cells and tissues. Previous studies into the utility of ultrasound for gene delivery used frequencies in the range of 20–50 kHz to induce cavitation (Fechheimer et al. 1987; Joersbo and Brunstedt 1990). In the process of cavitation, the ultrasonic field interacts with gas in the liquid leading to their growth and eventual implosion (Miller et al. 1996; Greenleaf et al. 1998). This collapse initiates shear stress, shock waves and microjets that affect the cells in the nearby vicinity (Unger et al. 2001). These effects lead to the permeability of the plasma membrane and reduce the thickness of the unstirred layer of the cell surface (Duvshani-Eshet et al. 2006). On the other hand,

Correspondence: K. Maruyama, Department of Pharmaceutical Sciences, School of Pharmaceutical Sciences, Teikyo University, 1091-1 Suwarashi, Sagami-hara, Sagami-hara, Kanagawa 229-0195, Japan. Tel: 81 42 685 3722. Fax: 81 42 685 3432. E-mail: maruyama@pharm.teikyo-u.ac.jp

these effects, if not properly controlled, induce the damages of tissue and cell (Ward et al. 1999). To overcome this problem, several studies have used frequencies of 1–3 MHz, intensities of 0.5–2 W/cm² and pulse-modulation (Lawrie et al. 1999; Duvshani-Eshet and Machluf 2005). In a separate approach, a combination of therapeutic ultrasound and microbubble echo contrast agents was shown to enhance gene transfection efficiency by effectively and directly transferring DNA into the cytosol (Shohet et al. 2000;

Li et al. 2003). Microbubbles based on protein microspheres and sugar microbubbles, are commercially available. However, the mean diameter of microbubbles is around 1.1–6 μm (Lindner 2004), it is too large for them to approach into peripheral tissues after intravascular injection. Therefore, microbubbles should generally be smaller than red blood cells.

Liposomes can be used as drug, antigen and gene delivery carriers: Their size can be easily controlled,

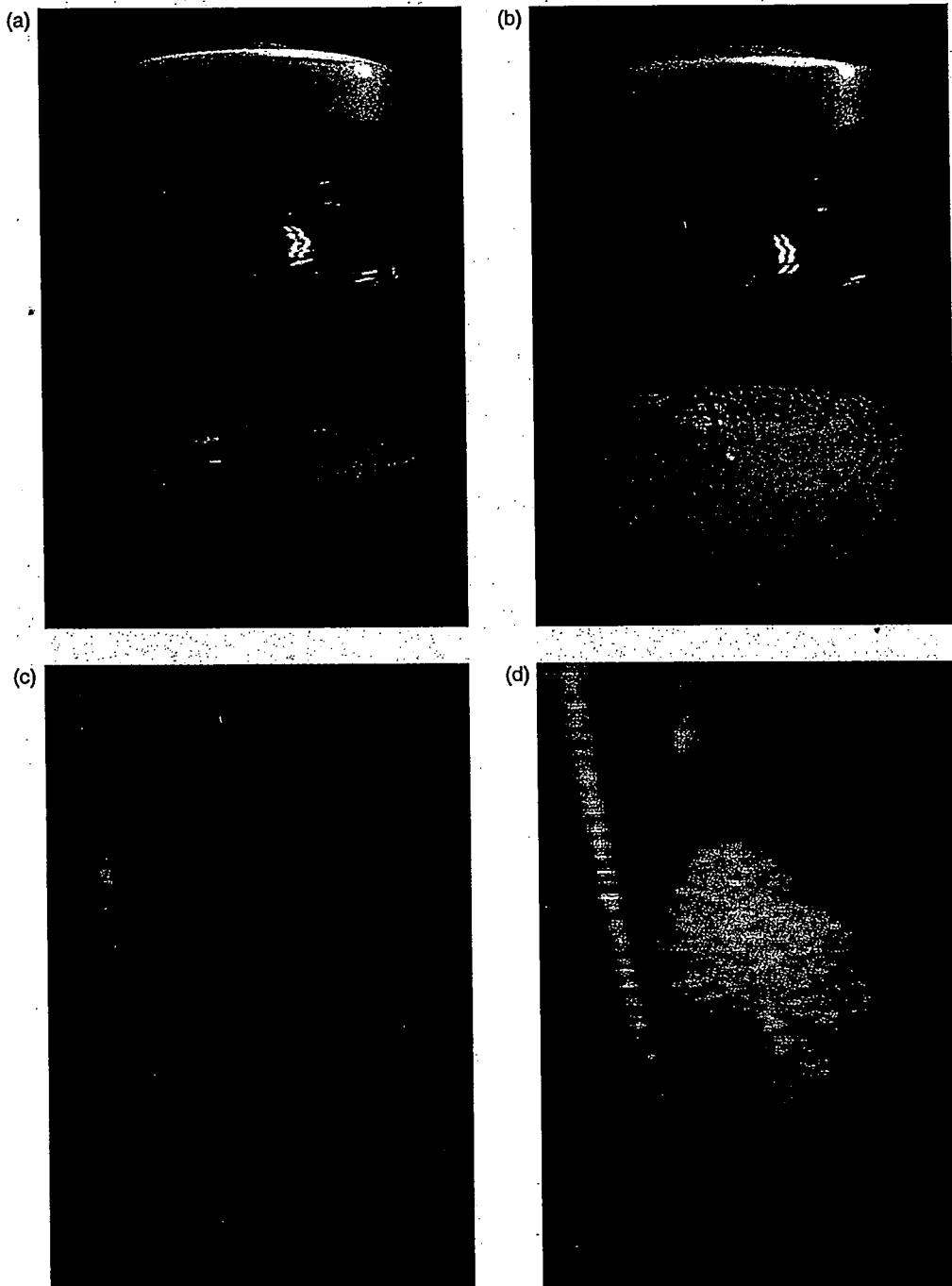


Figure 1. Aspect and ultrasonography of PEG-liposomes and Bubble liposomes. PEG-liposomes (a) were sonicated with supercharged perfluoropropane gas. After that, they became to Bubble liposomes (b). PEG-liposomes (c) and Bubble liposomes (d) were imaged with ultrasonography.

and they can be modified to add a targeting function (Harata et al. 2004; Kakudo et al. 2004; Kogure et al. 2004; Yanagie et al. 2004; Kawamura et al. 2006). Based on liposome technology, we developed Bubble liposomes as novel liposomal bubbles containing the ultrasound imaging gas, perfluoropropane (Suzuki et al. 2007). Bubble liposomes have a potential as ultrasound imaging agents. In addition, it is thought that Bubble liposomes can be used as novel gene delivery tools when they coupled with ultrasound exposure. In this review, we introduce about the feasibility of Bubble liposomes as imaging agents in ultrasonography and gene delivery tools utilized cavitation by ultrasound exposure.

Characteristics of Bubble liposomes

Bubble liposomes were made of polyethyleneglycol modified liposomes (PEG-liposomes) that were prepared with reverse phase evaporation method. PEG-liposomes placed in vials that were supercharged with perfluoropropane gas were sonicated in a bath sonicator (Suzuki et al. 2007). The suspension of Bubble liposomes became cloudier than the original liposome suspension (Figure 1(a),(b)). We confirmed whether the perfluoropropane gas was in fact trapped within the Bubble liposomes with ultrasound imaging (UF-750XT, Fukuda Denshi Co. Ltd, Tokyo, Japan). Echo signals were apparently enhanced in Bubble liposomes compared with conventional PEG-liposomes (Figure 1(c),(d)). These results showed that Bubble liposomes were including perfluoropropane gas. And we observed the Bubble liposomes with darklite illuminator (Nepa Gene Co. Ltd, Chiba, Japan) (Figure 2). In this study, we also observed Optison as conventional microbubbles. In the observation of Optison, most of microbubbles were more than 3 μm . Tsunoda et al. (2005) reported that the mean diameter of Optison particles is about 2.0–4.5 μm , they contain bubbles of up to 32 μm in

diameter. And some mice died immediately after the administration of Optison i.v. even without sonication due to lethal embolisms in vital organs. The same problem has not been reported in human, but there is possibility that Optison can not through capillary vessels. On the other hand, Bubble liposomes were smaller than Optison. Contrast microscopy showed that most of the Bubble liposomes were less than 3 μm in diameter. The mean diameter of Bubble liposomes was about 1 μm according to dynamic light scattering. Moreover, 500 μg of Bubble liposomes (in terms of lipid amount) injected into the tail veins of mice, did not cause any deaths (data not shown), indicating that these novel liposomal bubbles would be safe for use *in vivo*. Therefore, we expect that Bubble liposomes could access to deep tissues in organ. We are presently investigating the structure of Bubble liposomes by transmission electron microscopy.

Cardiosonography utilized with Bubble liposomes as imaging agents

Conventional microbubbles were mainly utilized as imaging agents in cardiosonography (Figure 3). In the ultrasound imaging of Bubble liposomes *in vitro*, echo signals was significantly increased. Therefore, it is thought that Bubble liposomes could also be utilized as ultrasound imaging agents. In this study, we assessed about the feasibility of Bubble liposomes as imaging agents in cardiosonography. When Bubble liposomes were injected into tail vein, the enhancement of echo signals was observed in the cardiac cavity. This enhancement was observed for about 5 min in the cavity. In addition, we also attempted to prepare the Bubble liposomes which were modified RGD peptide on the liposome surface for targeting to blood clotting site. These active targeting type of Bubble liposomes accumulated to blood clotting site in the blood clotting model rabbit. And we found out the blood clotting site with ultrasonography (data not shown). These results

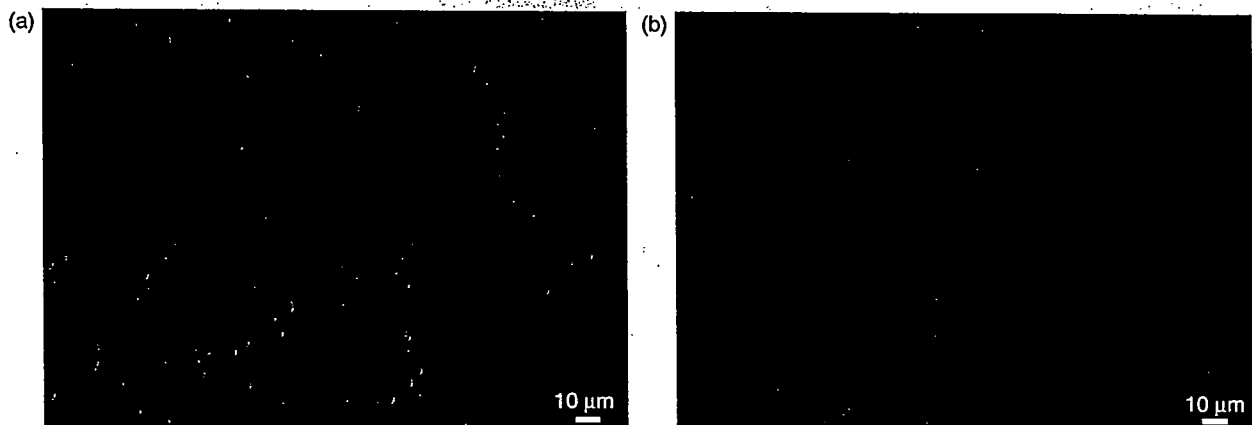


Figure 2. Microscopy of microbubbles and Bubble liposomes. (a) Microbubbles (Optison) and (b) Bubble liposomes were set on slide glasses and they were covered with cover glasses. The samples were observed with microscope under darklite illuminator.

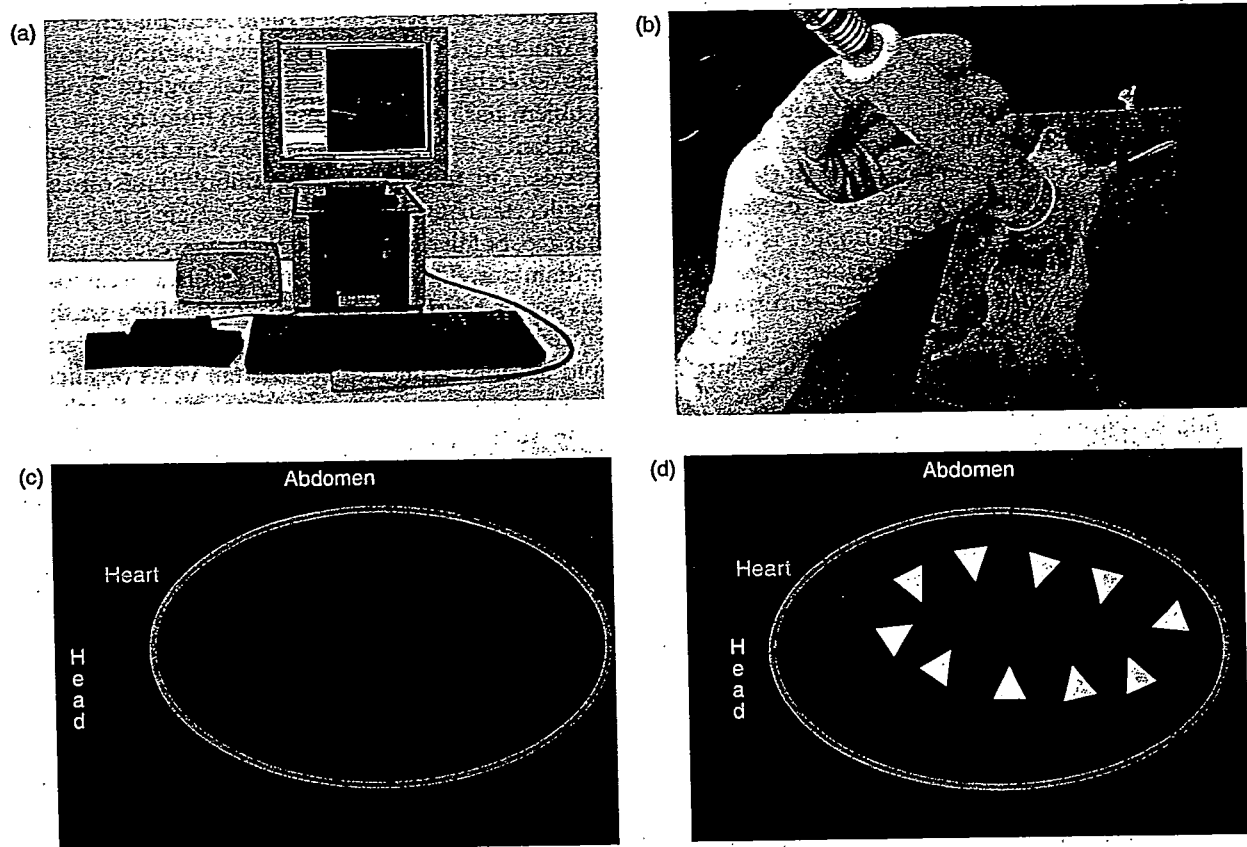


Figure 3. Cardiacsonography with Bubble liposomes. (a) Mouse was scanned with the probe (35 MHz) of ultrasonography before (b) or after injection of Bubble liposomes (100/100 μ l) into tail vein. Circle shows heart and triangle shows enhanced echo signals.

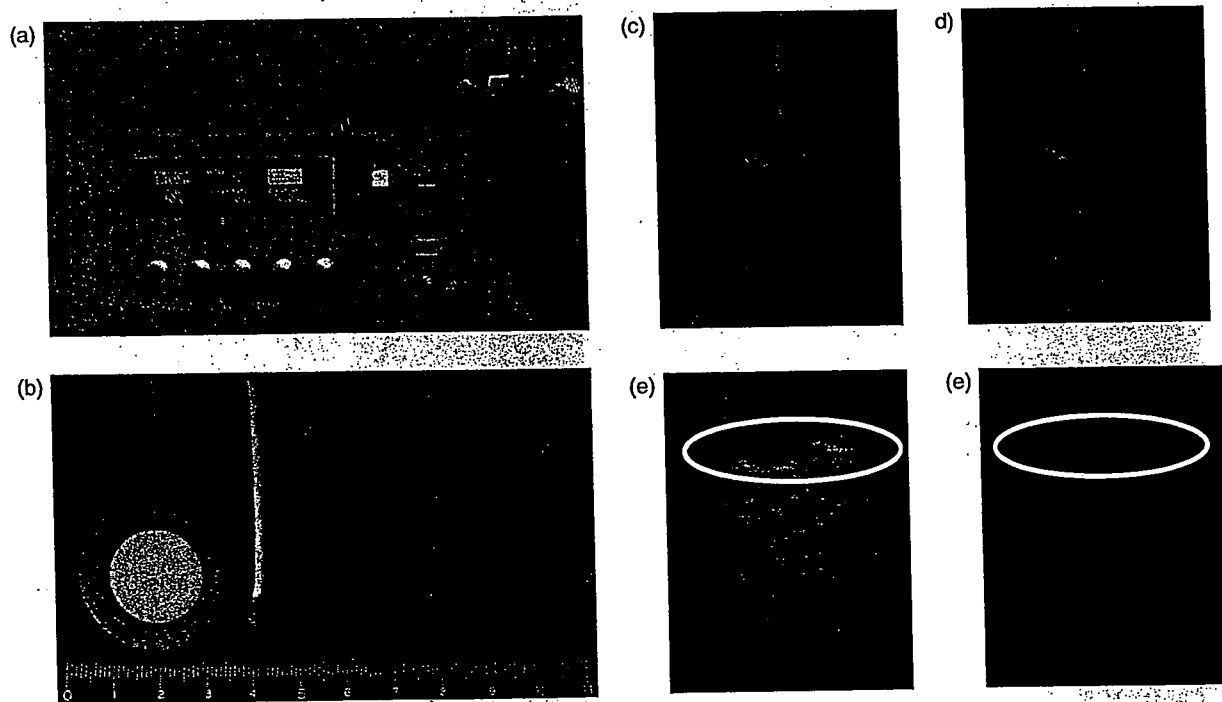


Figure 4. Cavitation of Bubble liposomes exposed with ultrasound. (a) Ultrasound generator. (b) Its probes. (c, d) Bubble liposomes were observed with naked image and (e, f) ultrasonography. The probe (circle) of ultrasound exposure was steeped in the suspension of Bubble liposomes. Then, they were exposed with ultrasound (2.5 W/cm^2) for 10 s. (c, e) Images were observed before (d, f) and after ultrasound exposure.

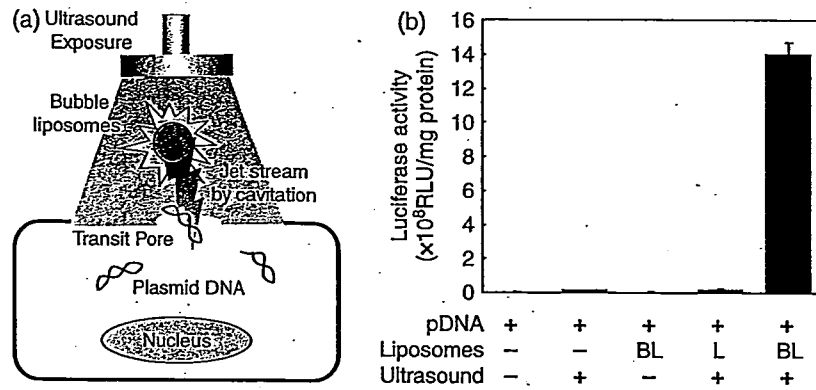


Figure 5. Gene delivery by the combination of Bubble liposomes and ultrasound. (a) Scheme of gene delivery by Bubble liposomes and ultrasound. When the ultrasound was exposed to Bubble liposomes, Bubble liposomes was induced cavitation. And the micro-jet stream was induced by the cavitation. The stream made the transit pore to the cell membrane. Then, extracellular plasmid DNA was delivered into cytosol. (b) Luciferase expression after transfection with Bubble liposomes and/or ultrasound. COS-7 cells (1×10^5 cells/500 μ l/tube) were mixed with pCMV-Luc (5 μ g) and Bubble liposomes (60 μ g). The cell mixture was exposed with ultrasound (Frequency, 2 MHz; Duty, 50%; Burst rate, 2 Hz; Intensity, 2.5 W/cm²; Time, 10 s). The cells were washed and cultured for 2 days. After that, luciferase activity was measured. Each data represents the mean \pm SD ($n = 3$). LB, Bubble liposomes; L, PEG-liposomes.

suggested that Bubble liposomes could be effective ultrasound imaging agents.

In vitro gene delivery with Bubble liposomes

Conventional microbubbles can induce cavitation when ultrasound is exposed to microbubbles (Li et al. 2003). The cavitation has the energy that is able to deliver extracellular molecules into cytosol (Taniyama et al. 2002). And so, we confirmed whether Bubble liposomes could induce cavitation by ultrasound exposure (Figure 4). Ultrasound was generated with Sonoporation Gene Transfection System (Figure 4(a),(b)) (Sonopore, Nepa Gene Co. Ltd, Chiba, Japan). After ultrasound exposure to Bubble liposomes, the suspension became clear (Figure 4(d)) and their ultrasound echo signals remarkably decreased (Figure 4(f)). This result suggested that cavitation was effectively induced by the combination of Bubble liposomes and ultrasound exposure. Thus, we assessed the feasibility of Bubble liposomes as gene delivery tools utilized with cavitation (Figure 5(a)). We examined the transduction of naked plasmid DNA into COS-7 cells by Bubble liposomes and/or ultrasound. Levels of luciferase expression were much higher after ultrasound in the presence, than in the absence of Bubble liposomes (Figure 5(b)). Amazingly, the gene expression efficiency was very high with the ultrasound exposure for 10 s though it was so short. We also confirmed that Bubble liposomes could effectively deliver plasmid DNA into cells even for 1 s of ultrasound exposure (data not shown). In addition, we examined the effect of ultrasound on cells with Bubble liposomes. Ultrasound did not remarkably affect the cells even when the amount of ultrasound was sufficient to induce cavitation of the Bubble liposomes (data not shown).

To evaluate the feasibility of Bubble liposomes as gene delivery tools, we examined about the transfection efficiency into various types of cells with Bubble liposomes and ultrasound. In this study, we attempted to deliver plasmid DNA into S-180 (mouse sarcoma), Colon26 (mouse colon adenocarcinoma), B16BL6 (mouse melanoma), Jurkat (human T cell line) and human umbilical vein endothelial cell (HUVEC) (Figure 6). The combination of Bubble liposomes and ultrasound more effectively transduced plasmid DNA into all of these cells than ultrasound alone. From these results, it was suggested that Bubble liposomes could deliver plasmid DNA into various types of cells.

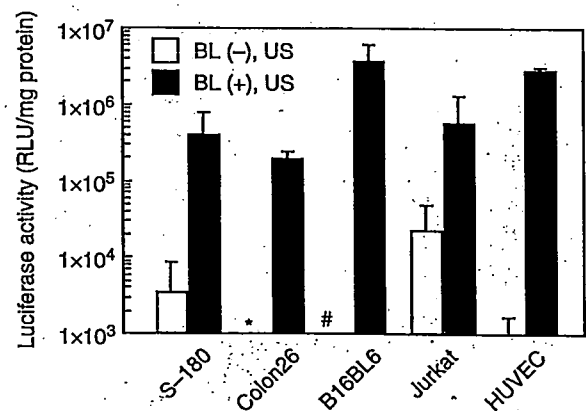


Figure 6. Luciferase expression in various types of cell transfected with Bubble liposomes and ultrasound. Cells (1×10^5 cells/500 μ l/tube) were mixed with pCMV-Luc (5 μ g) and Bubble liposomes (60 μ g). The cell mixture was exposed with or without ultrasound exposure (Frequency, 2 MHz; Duty, 50%; Burst rate, 2 Hz; Intensity, 2.5 W/cm²; Time, 10 s). The cells were washed and cultured for 2 days. After that, luciferase activity was measured. Each data represents the mean \pm SD ($n = 3$). BL, Bubble liposomes; US, Ultrasound. * $< 10^3$ RLU/mg protein, # $< 10^0$ RLU/mg protein.

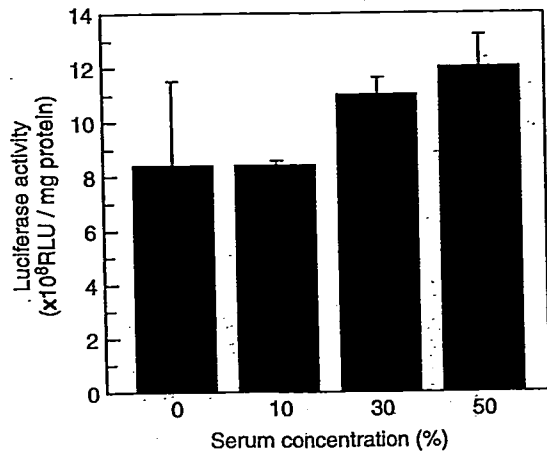


Figure 7. Effect of serum on transfection efficiency of Bubble liposomes. COS-7 cells (1×10^5 cells/500 μ l) mixed with pCMV-Luc (0.25 μ g) and Bubble liposomes (60 μ g) were exposed to ultrasound (Frequency, 2MHz; Duty, 50%; Burst rate, 2Hz; Intensity, 2.5 W/cm²; Time 10 s) in the absence or the presence of serum (0, 10, 30, 50%). The cells were washed and cultured for 2 days. Thereafter, luciferase activity was measured. Data are shown as means \pm SD ($n = 3$).

Considering *in vivo* gene delivery with Bubble liposomes, it is necessary to deliver plasmid DNA into cells in presence of serum (Figure 7). Then, we examined about the effect of serum on gene delivery with Bubble liposomes. Gene expression with Bubble liposomes was not affected even in the presence of serum. Therefore, Bubble liposomes would be novel gene delivery tools that could instantaneously transfect extracellular plasmid DNA into cells *in vivo*.

In vivo gene delivery with Bubble liposomes

To evaluate the ability of Bubble liposomes to *in vivo* gene delivery, we attempted to deliver plasmid DNA with Bubble liposomes into femoral artery (Figure 8). In this study, we also examined the gene delivery with conventional lipofection method. The gene expression with ultrasound or Bubble liposomes was low level. In addition, the gene expression was very low even in using Lipofectamine 2000. On the other hand, in the combination of Bubble liposomes and ultrasound exposure, gene expression was higher than other groups. And the gene expression was observed at only area of ultrasound exposure. These results suggested that Bubble liposomes could quickly deliver plasmid DNA into the artery by cavitation even under the condition of short contact time between Bubble liposomes and the endothelial cells and the existence of blood stream and serum. In this gene delivery system, it is thought that gene expression is transient (Suzuki et al. 2007). To maintain gene expression for long time, it is necessary to repeat injection. Fortunately, Bubble liposomes were made of PEG-liposomes which were very low immunogenic. Therefore, it is thought that we could repeat injection of Bubble liposomes without reducing the ability of gene delivery *in vivo*.

Conclusion

We prepared the liposomal bubbles that contained submicron-sized bubbles. These novel liposomes induced cavitation upon exposure to ultrasound, which resulted in plasmid DNA transduction into

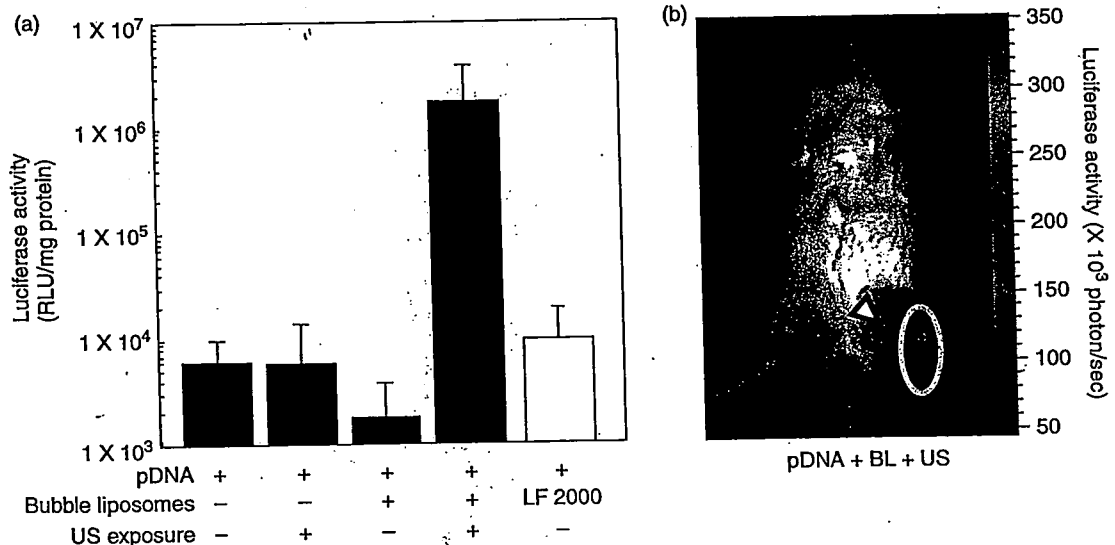


Figure 8. Gene delivery to femoral artery with Bubble liposomes. Each sample containing plasmid DNA (10 μ g) was injected into femoral artery. In the same time, ultrasound (Frequency, 1 MHz; Duty, 50%; Burst rate, 2 Hz; Intensity, 1 W/cm²; Time, 2 min) was exposed to the downstream area of injection site. (a) Luciferase expression in femoral artery of the ultrasound exposure area at 2 days after transfection. Data are shown as means \pm SD ($n = 5$). (b) *In vivo* luciferase imaging at 2 days after transfection in the mouse treated with plasmid DNA, Bubble liposomes and ultrasound exposure. The photon counts are indicated by the pseudo-color scales. Arrow head shows injection site and circle shows ultrasound exposure area. BL, Bubble liposomes; L, PEG-liposomes; LF2000, Lipofectamine2000; US, Ultrasound.

cells *in vitro* and *in vivo*. These results suggested that our Bubble liposomes will be useful tools for gene delivery as well as being a universal ultrasound imaging agent.

Acknowledgements

We are grateful to Dr Katsuro Tachibana (Department of Anatomy, School of Medicine, Fukuoka University) for technical advice regarding the induction of cavitation with ultrasound, to Dr Yasuhiro Matsu-mura (Investigative Treatment Division, Research Center for Innovative Oncology, National Cancer Center Hospital East) for technical advice regarding the gene delivery, to Mr Yasuhiko Hayakawa, Mr Takahiro Yamauchi and Mr Kosho Suzuki (Nepa Gene Co. Ltd) for technical advice regarding ultrasound exposure. This study was supported by an Industrial Technology Research Grant (04A05010) in 2004 from the New Energy and Industrial Technology Development Organization (NEDO) of Japan and a Grant-in-Aid for the Encouragement of Young Scientists (160700392) and the Exploratory Research (16650126) from the Japan Society for the Promotion of Science.

References

- Check E. 2002. Safety panel backs principle of gene-therapy trials. *Nature* 420:595.
- Check E. 2003. Second cancer case halts gene-therapy trials. *Nature* 421:305.
- Conwell CC, Huang L. 2005. Recent progress in non-viral gene delivery, p 3–10.
- Duvshani-Eshet M, Machluf M. 2005. Therapeutic ultrasound optimization for gene delivery: A key factor achieving nuclear DNA localization. *J Control Release* 108:513–528.
- Duvshani-Eshet M, Adam D, Machluf M. 2006. The effects of albumin-coated microbubbles in DNA delivery mediated by therapeutic ultrasound. *J Control Release* 112:156–166.
- Fechheimer M, Boylan JF, Parker S, Siskin JE, Patel GL, Zimmer SG. 1987. Transfection of mammalian cells with plasmid DNA by scrape loading and sonication loading. *Proc Natl Acad Sci USA* 84:8463–8467.
- Greenleaf WJ, Bolander ME, Sarkar G, Goldring MB, Greenleaf JF. 1998. Artificial cavitation nuclei significantly enhance acoustically induced cell transfection. *Ultrasound Med Biol* 24: 587–595.
- Harata M, Soda Y, Tani K, Ooi J, Takizawa T, Chen M, Bai Y, Izawa K, Kobayashi S, Tomonari A, Nagamura F, Takahashi S, Uchimaru K, Iseki T, Tsuji T, Takahashi TA, Sugita K, Nakazawa S, Tojo A, Maruyama K, Asano S. 2004. CD19-targeting liposomes containing imatinib efficiently kill Philadelphia chromosome-positive acute lymphoblastic leukemia cells. *Blood* 104:1442–1449.
- Joersbo M, Brunstedt J. 1990. Protein synthesis stimulated in sonicated sugar beet cells and protoplasts. *Ultrasound Med Biol* 16:719–724.
- Kakudo T, Chaki S, Futaki S, Nakase I, Akaji K, Kawakami T, Maruyama K, Kamiya H, Harashima H. 2004. Transferrin-modified liposomes equipped with a pH-sensitive fusogenic peptide: An artificial viral-like delivery system. *Biochemistry* 43: 5618–5628.
- Kawamura K, Kadowaki N, Suzuki R, Udagawa S, Kasaoka S, Utoguchi N, Kitawaki T, Sugimoto N, Okada N, Maruyama K, Uchiyama T. 2006. Dendritic cells that endocytosed antigen-containing IgG-liposomes elicit effective antitumor immunity. *J Immunother* 29:165–174.
- Kogure K, Moriguchi R, Sasaki K, Ueno M, Futaki S, Harashima H. 2004. Development of a non-viral multifunctional envelope-type nano device by a novel lipid film hydration method. *J Control Release* 98:317–323.
- Lawrie A, Brisken AF, Francis SE, Tayler DI, Chamberlain J, Crossman DC, Cumberland DC, Newman CM. 1999. Ultrasound enhances reporter gene expression after transfection of vascular cells *in vitro*. *Circulation* 99:2617–2620.
- Lindner JR. 2004. Microbubbles in medical imaging: Current applications and future directions. *Nat Rev Drug Discov* 3: 527–532.
- Li T, Tachibana K, Kuroki M, Kuroki M. 2003. Gene transfer with echo-enhanced contrast agents: Comparison between albumex, optison, and levovist in mice—initial results. *Radiology* 229: 423–428.
- Marshall E. 1999. Gene therapy death prompts review of adenovirus vector. *Science* 286:2244–2245.
- Miller MW, Miller DL, rayman AA. 1996. A review of *in vitro* bioeffects of inertial ultrasonic cavitation from a mechanistic perspective. *Ultrasound Med Biol* 22:1131–1154.
- Mizuguchi H, Nakagawa T, Nakanishi M, Imazu S, Nakagawa S, Mayumi T. 1996. Efficient gene transfer into mammalian cells using fusogenic liposome. *Biochem Biophys Res Commun* 218: 402–407.
- Shohet RV, Chen S, Zhou YT, Wang Z, Meidell RS, Unger RH, Grayburn PA. 2000. Echocardiographic destruction of albumin microbubbles directs gene delivery to the myocardium. *Circulation* 101:2554–2556.
- Suzuki R, Takizawa T, Negishi Y, Hagiwara K, Tanaka K, Sawamura K, Utoguchi N, Nishioka T, Maruyama K. 2007. Gene delivery by combination of novel liposomal bubbles with perfluoropropane and ultrasound. *J Control Release* 117: 130–136.
- Taniyama Y, Tachibana K, Hiraoka K, Namba T, Yamasaki K, Hashiya N, Aoki M, Ogihara T, Yasufumi K, Morishita R. 2002. Local delivery of plasmid DNA into rat carotid artery using ultrasound. *Circulation* 105:1233–1239.
- Tsunoda S, Mazda O, Oda Y, Iida Y, Akabane S, Kishida T, Shin-Ya M, Asada H, Gojo S, Imanishi J, Matsubara H, Yoshikawa T. 2005. Sonoporation using microbubble BR14 promotes pDNA/siRNA transduction to murine heart. *Biochem Biophys Res Commun* 336:118–127.
- Unger EC, Hersh E, Vannan M, McCreery T. 2001. Gene delivery using ultrasound contrast agents. *Echocardiography* 18: 355–361.
- Wada K, Arima H, Tsutsumi T, Chihara Y, Hattori K, Hirayama F, Uekama K. 2005. Improvement of gene delivery mediated by mannosylated dendrimer/alpha-cyclodextrin conjugates. *J Control Release* 104:397–413.
- Ward M, Wu J, Chiu JF. 1999. Ultrasound-induced cell lysis and sonoporation enhanced by contrast agents. *J Acoust Soc Am* 105:2951–2957.
- Yanagie H, Ogura K, Takagi K, Maruyama K, Matsumoto T, Sakurai Y, Skvarc J, Illic R, Kuhne G, Hisa T, Yoshizaki I, Kono K, Furuya Y, Sugiyama H, Kobayashi H, Ono K, Nakagawa K, Eriguchi M. 2004. Accumulation of boron compounds to tumor with polyethylene-glycol binding liposome by using neutron capture autoradiography. *Appl Radiat Isot* 61:639–646.

Antitumor effect of TNP-470, an angiogenesis inhibitor, combined with ultrasound irradiation for human uterine sarcoma xenografts evaluated using contrast color Doppler ultrasound

Makoto Emoto,^{1,4} Katsuro Tachibana,² Hiroshi Iwasaki³ and Tatsuhiko Kawarabayashi¹

Departments of ¹Obstetrics and Gynecology, ²Anatomy, and ³Pathology, Fukuoka University Medical School, Fukuoka 814-0180, Japan

(Received January 9, 2007/Revised February 8, 2007/Accepted February 21, 2007/Online publication April 6, 2007)

Microvascular endothelial cells, which are recruited by tumors, have become an important target in cancer therapy. This study firstly examined the antitumor effect of angiogenesis inhibitor combined with ultrasound (US) irradiation for human cancer *in vivo* and evaluated its vascularity using color Doppler US in real time with a microbubble US contrast agent. A human uterine sarcoma cell line, FU-MMT-1, was used *in vivo* because this tumor is one of the most malignant neoplasms of the human solid tumors and it also has a poor response to any of the chemotherapeutic agents currently used, as well as to radiotherapy. In angiogenic inhibitors, TNP-470 was selected to use in an *in vivo* study, because this agent showed a higher inhibitory effect in tube formation assay *in vitro*, than that of FR118487, or thalidomide. The FU-MMT-1 xenografts in nude mice were treated using US at a low-intensity (2.0 w/cm², 1MHZ) for 4 min three times per week each after the subcutaneous injection of TNP-470 (30 mg/kg), an angiogenesis inhibitor, and this treatment was continued for 8 weeks. Either treatment of US alone or TNP-470 alone showed a suppression of tumor growth, in comparison to the non-treatment group (control), and a significantly enhanced effect was obtained using the combined treatment. A reduction in the intratumoral vascularity, which was evaluated using both color Doppler and immunohistochemistry, was significantly demonstrated using the combined treatment, in comparison to each treatment alone, and the control. No side-effect was observed in any mice in the combined treatment group. These results suggest that the antitumor effect of TNP-470 for uterine sarcoma was accelerated by US irradiation *in vivo* and this combination might be a potentially effective for new cancer therapy. (*Cancer Sci* 2007; 98: 929-935)

Angiogenesis, the growth of new capillary blood vessels from pre-existing vasculature, is a crucial process for tumor progression and metastasis.⁽¹⁾ The microvascular endothelial cells (EC), which are recruited by tumors, have thus become an important second target in cancer therapy.⁽²⁾ Angiogenesis inhibitors have thus been developed to target vascular EC and block tumor angiogenesis. Anti-angiogenic therapy alone has been shown to be able to suppress the growth of established tumors and a recent clinical trial showed successful results for advanced rectal cancer.⁽³⁾ The addition of antiangiogenic agents to chemotherapy,^(4,5) radiation,^(6,7) or molecular-targeting agents has thus been suggested to potentially increase clinical efficacy. Gorski *et al.* showed that radiotherapy and antibodies against VEGF had a synergistic effect against primary tumors.⁽⁶⁾ According to an analysis of a bibliographic database, MEDLINE, however, no previous study has ever examined the combination of angiogenesis inhibitors and ultrasound (US) irradiation in the field of cancer research.

O-(chloroacetyl-carbamoyl)fumagillol (TNP-470) is a low-molecular-weight synthetic analog of fumagillin, a natural

compound secreted by the fungus *Aspergillus fumigatus fresenius*.⁽⁸⁾ TNP-470 blocks endothelial cell cycle progression in the late G1 phase by activating p53 through a mechanism leading to cyclin-dependent kinase inhibitor p21^{CIP/WAF} expression.⁽⁹⁾ The cellular target of TNP-470 was found to be methionine aminopeptidase-2 (MetAP-2), an intracellular enzyme necessary for the process of protein myristylation.⁽¹⁰⁾ The antitumor effect of TNP-470 has been shown in various tumors of human malignancies both *in vitro* and *in vivo*.⁽¹¹⁻¹³⁾ Our previous studies have shown that TNP-470 inhibited the VEGF production and proliferation of a uterine sarcoma cell line, FU-MMT-1, *in vitro*⁽¹³⁾ which had been established from a patient with uterine carcinosarcoma.⁽¹⁴⁾ The combination of TNP-470 and cytotoxic agents^(4,5) or radiation⁽¹⁵⁾ has showed a successful outcome *in vivo*.

US has been shown to enhance the antitumor effect of a chemotherapeutic agent *in vitro* and *in vivo*.⁽¹⁶⁻¹⁹⁾ Transiently increased permeability of the cell membrane is one of the mechanisms of the US-enhanced chemotherapy.⁽²⁰⁾ Sonoporation, and resealing of the cell membrane by acoustic pressure are considered to be a primary reason for an increased intracytoplasmic concentration of the administered agent.⁽²¹⁾ Ablation of adult T-cell leukemia cells and lysis of HL-60 cells by low-intensity US is enhanced in the presence of a photosensitizing drug, indicating that the photosensitive drug potentiates the cytotoxicity of US.^(21,22) The potentiation of some anticancer agents occurs when the agent may become more potent against the tumor cells when used in conjunction with US. The absorption of ultrasound energy by the agent and the production of free radicals seem to be the likely mechanisms of this increase.^(23,24) In order to assess the accelerated (synergistic) drug effect of angiogenesis inhibitor using US energy, this study examined for the first time the therapeutic effect of an angiogenesis inhibitor combined with US irradiation for human cancer *in vivo*. In addition, the effect of antiangiogenesis in this combined treatment was assessed non-invasively using color Doppler US in real-time with a microbubble contrast agent.

Materials and Methods

Cell line and nude mice. A human uterine sarcoma cell line, FU-MMT-1, previously established by us from a patient with uterine carcinosarcoma, was used in this study because this tumor is one of the most malignant neoplasms of the human solid tumors and it also has a poor response to any of the chemotherapeutic agents currently used, as well as to radiotherapy. FU-MMT-1 shows highly progressive activity both *in vitro* and *in vivo*. This

*To whom correspondence should be addressed. E-mail: emoto@cis.fukuoka-u.ac.jp

cell line is chiefly composed of rhabdomyosarcoma cells and the immunophenotype, tumorigenicity, and cytogenetic characteristics have been reported previously.⁽¹⁴⁾ Female BALB/cA Jcl-nu athymic nude mice were obtained from Clea (Tokyo, Japan). Five to 6-week-old mice weighing 20 g were used in the experiments. All animals were kept in isolation rooms at a controlled temperature and they were caged in groups of five or fewer and had free access to standard animal chow and water according to the Instructions of the Institute of Experimental Animal Science, Fukuoka University Medical School.

In vitro tube formation assay. Experiments on tube formation were conducted in triplicate in 24-multiwell dishes using an Angiogenesis kit (Kurabo, Osaka, Japan), according to the manufacturer's instructions. Briefly, human umbilical vein endothelial cells (HUVEC) cocultured with human fibroblasts were cultivated with TNP-470 (1 µg/mL), FR118487 (1 µg/mL), and thalidomide (1 µg/mL) in the medium containing 10 ng/mL of vascular endothelial growth factor (VEGF). An angiogenesis inhibitor, FR118487 was synthesized by chemical modification of the fermentation products of a fungus, *Scolecobasidium arenarium* (F-2015), at Fujisawa Pharmaceutical Co., Ltd (Tsukuba, Japan). The medium was changed every 3 days. After 10 days, the dishes were washed with phosphate-buffered saline (PBS) and fixed with 70% ethanol at 4°C. After the fixed cells were rinsed three times with PBS, the cells were then incubated with mouse antihuman CD31 (Kurabo, Osaka, Japan) in PBS containing 1% bovine serum albumin (BSA) for 60 min. After washing with 1% BSA-PBS three times, the cells were incubated with goat antimouse IgG AikP conjugate (Kurabo, Osaka, Japan). Metal-enhanced 3,3'-diamino-benzidine-tetrahydrochloride (DAB) was the substrate, the reaction yielding a dark reddish-brown insoluble end-product. Finally, the cells were washed with PBS five times, and viewed using an Olympus microscope. The area and tube length were measured using the Kurabo angiogenesis image analyzer (Kurabo, Osaka, Japan) in five different fields per each well, and then were statistically analyzed.

Chemicals. TNP-470 was kindly donated by Takeda Chemical Industries (Osaka, Japan). Its structure and characteristics have been described previously.⁽¹¹⁾ TNP-470 was suspended in a vehicle of 0.5% ethanol plus 5% gum arabic in saline. FR118487 was kindly donated by Fujisawa Pharmaceutical Co., Ltd (Tsukuba, Japan). The inhibitory effect of this drug on angiogenesis in the rabbit cornea has previously been described.⁽²⁵⁾

Injection of TNP-470 and ultrasound irradiation. The mice were injected subcutaneously with 2×10^5 FU-MMT-1 cells in 0.2 mL DMEM in the right auxiliary region of the flank. Mice bearing the resultant tumors measuring 5–10 mm in diameter on the 14th day were randomly separated into four groups as follows: i) US irradiation alone ($n = 8$); ii) TNP-470 injection alone ($n = 8$); iii) combination of TNP-470 and US irradiation ($n = 8$), and iv) non-treatment as the control ($n = 12$: injection of 0.5% ethanol plus 5% gum arabic in saline) and these therapies were continued for 8 weeks. TNP-470 was injected subcutaneously at a dose of 30 mg/kg three times per week for each mouse in groups of TNP-470 alone and the combined treatment. The mice were anesthetized with ether and US (continuous wave, at 1 MHz frequency, and 2.0 w/cm² intensity), was irradiated through a probe onto subcutaneous tumors for 4 min three times per week using Sonitron 1000 (Rich-mar, Inola, OK) for each mouse in groups of US alone and the combined treatment. Tumor growth was monitored by measuring the weekly volume twice, calculated as $V = a \times b^2/2$ (a = length; b = width). An autopsy was done on all mice soon after finishing these therapies or when they died during the course of therapies and the tumors were then harvested, and the size and the weights of these tumors were measured. Mean, SD, median, and SE of the tumor size during the courses and those of the tumor weight after the therapies in each group were calculated.

Evaluation of tumor vascularity with contrasted color Doppler US.

The intratumoral vascularity in xenografts was examined after finishing each treatment using color Doppler US (SSD-4000, Aloka Ltd, Tokyo, Japan) with a 7.5-MHz curved array transducer (UST-987-7.5, Aloka Ltd) using a microbubble ultrasound contrast agent, Optison® (Molecular Biosystems Inc., San Diego, CA, USA) at our animal center in Fukuoka University. The US examinations were standardized using a medium wall filter, pulsed repetition frequency of 1000 Hz, moderate-to-long persistence, and a slow and steady movement of the transducer to achieve the highest sensitivity without apparent background noise. The intratumoral blood flow was enhanced after an i.v. bolus injection of Optison® (0.6 mL/kg). Optison® is approved for use in echocardiography by the USA Food and Drug Administration (FDA) and consists of a suspension of perfluoropropane-filled albumin microspheres with a concentration of 6.3×10^8 bubbles/mL. After the examination, the previously stored images were retrieved and displayed on the monitor. The area in the longitudinal image on the US monitor of each tumor was automatically calculated using the manual-trace measurement of the length of tumor circumference, then, the number of colored vessels within the tumor was counted. The average sonographic vascular density (ASVD) was calculated as the number of colored-vessels within a longitudinal tumor section divided by the area. The ASVD in each treatment group was calculated (\pm SD) and statistically compared. Moreover, the areas of highest neovascularization were then identified on their stored images. The tumor vessel counts over an area of 19.625-mm² (a field of a circle with 5 mm in diameter) per field in each of these three areas within the tumor were then counted as the highest sonographic vascular density (HSVD). The averages of the HSVD in the three 19.625-mm² fields of each tumor were calculated in each treatment group (\pm SD) and statistically compared.

Evaluation of tumor vascularity with immunohistochemistry. The paraffin sections from each tumor were reacted with each primary antibody for 1 h at room temperature in our pathology laboratory. The attached antibodies were visualized using the labeled streptavidin-biotin (LSAB) method (Zymed, San Francisco, CA, USA). The monoclonal antibody used was anti-CD34 (an endothelial marker: 1:50; Dako) for endothelial cells in the tumor vessels. The negative controls consisted of an omission of the primary antibody. Microvessel density (MVD) was measured in all tumors treated in this therapy. Intratumoral microvessels were highlighted using anti-CD34 immunostaining in formalin-fixed, paraffin-embedded sections in each tumor. The MVD quantitation in the highest vascularization (so-called hot spots) was examined in each tumor in the same manner as in our previous study,⁽²⁶⁾ which was named as the highest immunohistochemical MVD (HIMVD). The average of the HIMVD in these three groups and that in the controls was then calculated. Moreover, to assess the average vascularization in entire tumor sections, 10 areas were randomly chosen in each tumor then the tumor vessels were counted, and then the obtained density was considered to be the average immunohistochemical MVD (AIMVD).

Statistical analysis. These *in vivo* data were expressed as the mean \pm SD. The Mann-Whitney *U*-test (non-parametric) was used to compare tumor growth, or tumor weight between three treatment groups and the control. The unpaired *t*-test (parametric) was used to compare tumor vessel density between three treatment groups and the control. These statistical analyses were done using the software package StatView 5.0 (SAS Institute, Inc., Cary, NC, USA) for Macintosh. The results were judged to be statistically significant if the *P*-value of each respective test statistic was less than 0.0001.

Results

In vitro tube formation assay. To investigate the antiangiogenic effect of angiogenesis inhibitors, a tube formation assay was

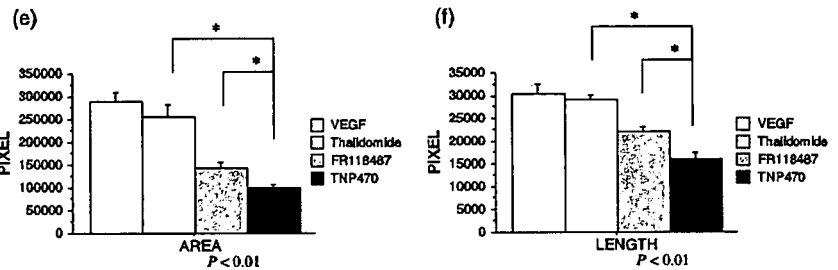
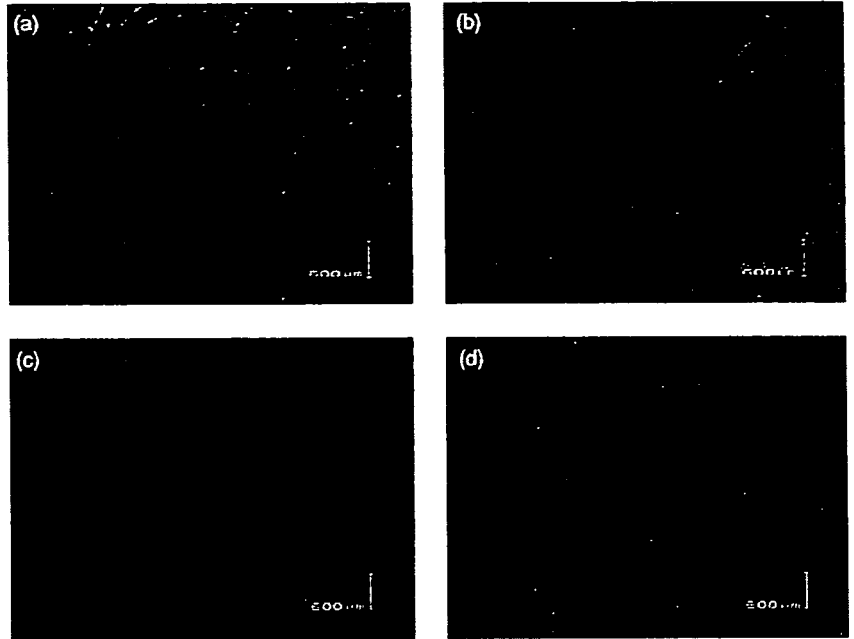


Fig. 1. (a–f) Effects on tube formation *in vitro*. (a) When human umbilical vein endothelial cells (HUVEC) were cultured in the presence of VEGF (10 ng/mL), efficient tube formation was observed. (d) TNP-470 (1 μg/mL) significantly inhibited the tube formation *in vitro*, in comparison to the other two antiangiogenic agents, (b) thalidomide (1 μg/mL) and (c) FR118487 (1 μg/mL), in quantitative analysis of both (e) tube area and (f) length using an image analyzer.

performed using HUVEC cocultured with human fibroblasts. When HUVEC were cultured in the presence of VEGF, efficient tube formation was observed (positive control). In a quantitative analysis of both tube area and length, TNP-470 significantly inhibited the tube formation *in vitro*, in comparison to the other two antiangiogenic agents, thalidomide, and FR118487 in this study ($P < 0.01$; Fig. 1a–f). We therefore finally selected TNP-470 to use in our following *in vivo* study as a representative agent.

Suppression of tumor growth. The weekly changes in the mean tumor volume in xenografts during the courses of therapies are shown in Fig. 2. Either treatment of US alone or TNP-470 alone inhibited the growth of the FU-MMT-1 xenografts, in comparison to that of the control (Mann–Whitney-*U*-test: $P = 0.151$, and $P = 0.006$). Furthermore, a significantly enhanced effect to suppress the tumor growth was obtained using the combined treatment (vs US alone: $P < 0.0001$; and vs TNP-470 alone: $P < 0.0001$; Fig. 1). No significant difference in the mean tumor volume was observed between the treatments using US alone and TNP-470 alone ($P = 0.176$).

The mean weight after treatment of either US alone (10.98 ± 2.27 g, range: 4.8–17.2 g) or TNP-470 alone (8.94 ± 3.07 g, range: 0.0–21.2 g) was smaller than that of the control (Mann–Whitney-*U*-test vs US alone: $P = 0.0042$; vs TNP-470 alone: $P = 0.025$). The enhanced effect of the weight reduction in xenografts was shown by the combined treatment (0.75 ± 0.52 g, range: 0.0–4.8 g), in comparison to either US alone ($P = 0.027$) or TNP-470 alone ($P = 0.050$). The mean weight of the xenografts measured after the combined treatment was significantly lower than that of the control (25.04 ± 3.85 g, range: 7.6–30.8 g; $P = 0.0007$; Fig. 3).

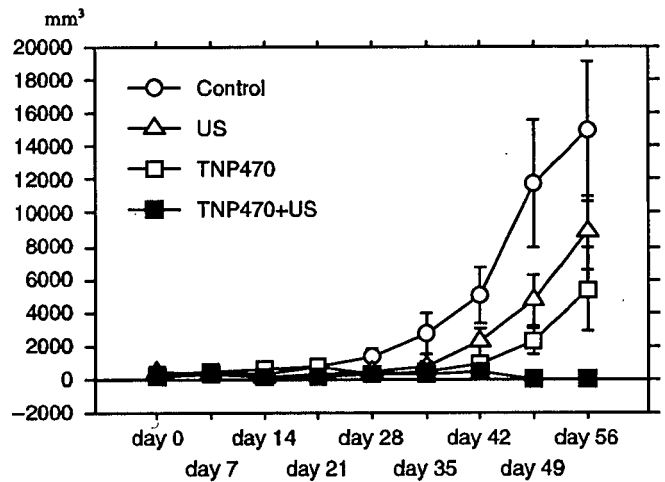


Fig. 2. Effects on growth of the FU-MMT-1 xenografts. Each curve represents the mean and SD of the tumor (mm³) volume in each group. Either treatment with ultrasound alone or TNP-470 alone significantly inhibited the growth of the FU-MMT-1 xenografts, in comparison to that of the non-treatment group (control; Mann–Whitney-*U*, $P = 0.151$, and $P = 0.006$). Moreover, a significantly enhanced effect was obtained using the combined treatment, in comparison to that of each therapy alone (Mann–Whitney-*U*, vs US alone: $P < 0.0001$, and vs TNP-470 alone: $P < 0.0001$).

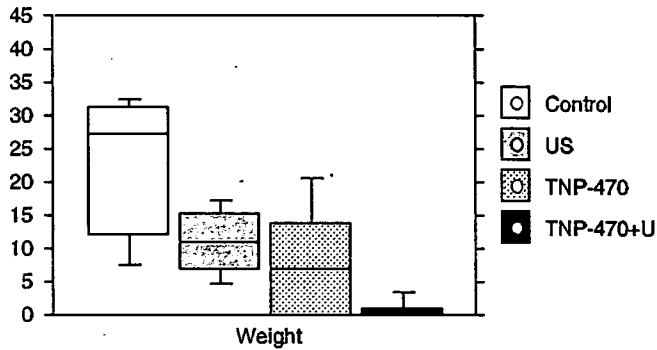


Fig. 3. The mean (SD) tumor weights (g) in the FU-MMT-1 xenografts resected after treatment. The mean tumor weight after treatment of either ultrasound (US) alone (10.98 ± 2.27 g, range: 4.8–17.2 g) or TNP-470 alone (8.94 ± 3.07 g, range: 3.1–21.2 g) was smaller than that of the control (25.04 ± 3.85 g, range: 7.6–30.8 g; Mann-Whitney-*U*-test, vs US alone: $P = 0.0042$; vs TNP-470 alone; $P = 0.025$). The enhanced effect of the weight reduction in xenografts was shown by the combined treatment (0.75 ± 0.52 g, range: 0.0–4.8 g), in comparison to either US alone ($P = 0.027$) or TNP-470 alone ($P = 0.050$). The mean tumor weight of the xenografts measured after the combined treatment was significantly lower than that of the control ($P = 0.0007$).

After these treatments, disappearance of the tumor (tumor free) was seen in five of eight (62.5%) mice in the combined treatment, and two of eight (25.0%) in TNP-470 alone (χ^2 test; $P = 0.13$), whereas no such disappearance was seen after US alone, or in the control (vs combined treatment: $P = 0.007$, and $P = 0.001$). Dissemination, or direct invasion into the abdominal cavity by the tumor was only seen in the control (33.3%; four of 12 mice).

Evaluation of the antiangiogenic effect using contrast color Doppler ultrasound. The effects of antiangiogenesis for FU-MMT-1 xenografts by these therapies were evaluated using contrast Doppler US in real-time after the 8 weeks of treatment (Fig. 4a–d). In the evaluation with ASVD, the mean of the group of combination treatment was significantly lower than that of the control (unpaired *t*-test: $P = 0.04$), whereas no significant difference was observed between either the treatment of US alone or TNP-470 alone and the control ($P = 0.39$, $P = 0.41$). In the evaluation with HSVD, the mean of the group of either TNP alone or combination treatment was thus significantly lower than that of the control (unpaired *t*-test: $P = 0.002$, $P = 0.000004$), whereas no significant difference was observed between the treatment of US alone and the control ($P = 0.16$). The reduction in the vascular density (HSVD) was significantly enhanced by the combined treatment, in comparison to that of the US treatment alone ($P = 0.0003$), or the TNP-470 alone ($P = 0.00009$; Table 1). The intratumoral vascularity could not be fully evaluated

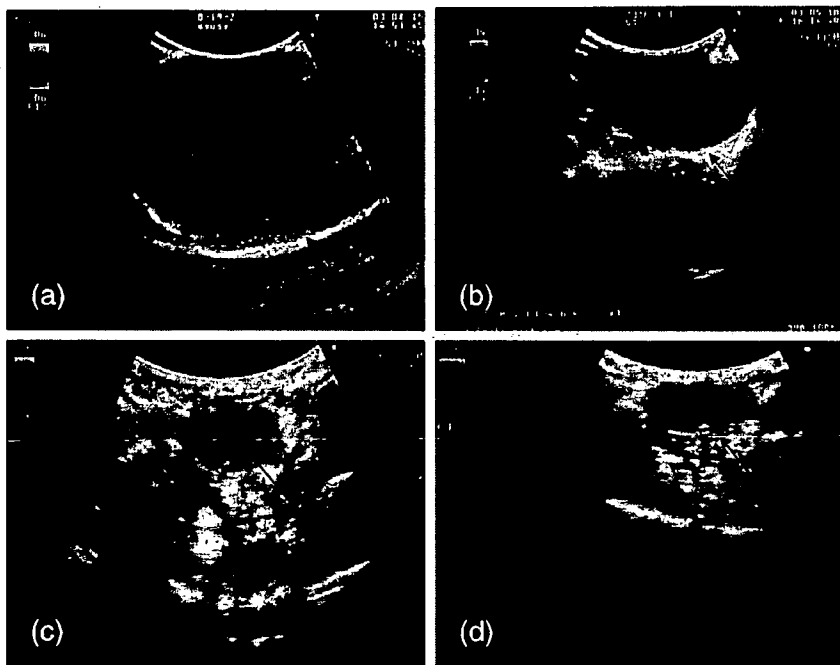


Fig. 4. (a–d) Visualization of the intratumoral blood flow using non-invasive contrasted color Doppler ultrasound (US) in FU-MMT-1 human uterine sarcoma growing subcutaneous on the backs of BALB/cA Jcl-nu mice. Representative Doppler ultrasound pictures are taken at maximal signal intensity after injecting the US contrast agent (10 s after injection). The tumor vessel density in (c) the group of TNP-470 treatment alone was lower than that of (a) the control (unpaired *t*-test, $P = 0.0007$), whereas no significant difference was observed between (b) the treatment of US alone and the control (unpaired *t*-test, $P = 0.11$). The reduction of tumor vessel density was significantly enhanced by (d) the combined treatment, in comparison to that of the US treatment alone ($P = 0.00002$), or the TNP-470 alone (unpaired *t*-test, $P = 0.00009$).

Table 1. The sonographic and immunohistochemical vascular density in FU-MMT-1 xenografts after 8 weeks' treatments

	Control	US alone	TNP-470 alone	TNP-470 + US
1) Average sonographic vascular density (per 100 mm ²)	8.6 ± 2.1	7.7 ± 2.0	7.6 ± 2.3	5.5 ± 1.3
2) Highest sonographic vascular density (per 19.63 mm ²)	14.6 ± 1.8	12.9 ± 2.7	11.1 ± 1.4	3.6 ± 1.1
3) Average immunohistochemical microvessel density†	49.8 ± 10.2	25.9 ± 12.1	25.1 ± 14.1	9.4 ± 3.2
4) Highest immunohistochemical microvessel density†	61.3 ± 10.7	60.8 ± 14.7	50.8 ± 13.7	11.3 ± 2.2

†Per high-power field (0.74 mm²). 1) Control versus US: $P = 0.39$, or TNP-470: $P = 0.41$, or TNP-470 + US: $P = 0.04$. TNP-470 versus TNP-470 + US: $P = 0.19$. 2) Control versus US: $P = 0.16$, or TNP-470: $P = 0.002$, or TNP-470 + US: $P = 0.000004$. TNP-470 + US versus US alone: $P = 0.0003$, or TNP-470: $P = 0.00009$. 3) Control versus US: $P = 0.0008$, or TNP-470: $P = 0.002$, or TNP-470 + US: $P = 0.0001$. TNP-470 + US versus US alone: $P = 0.05$, or $P = 0.04$. 4) Control versus US: $P = 0.94$, or TNP-470: $P = 0.13$, or TNP-470 + US: $P = 0.000002$. TNP-470 + US versus US alone: $P = 0.0001$, or TNP-470 alone: $P = 0.001$. Bald: $P < 0.05$ (versus control).

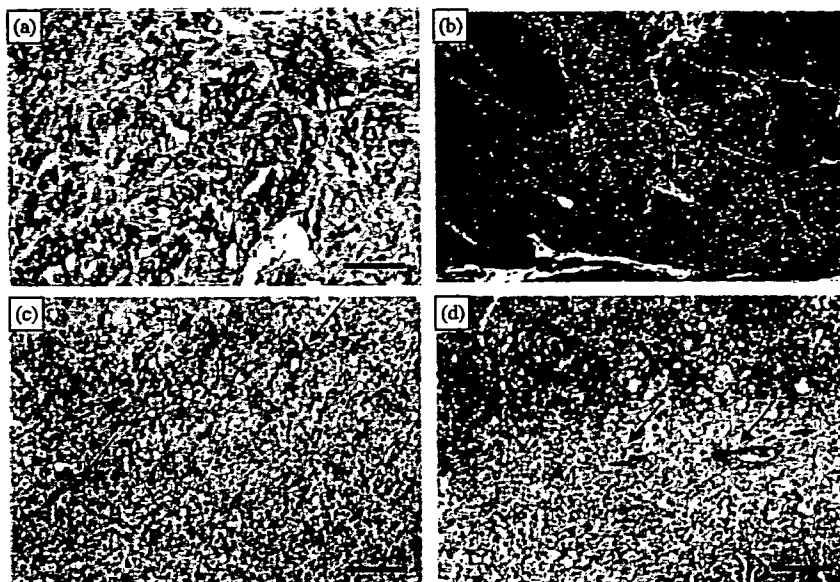


Fig. 5. (a–d) Intratumoral microvessels immuno-histochemically stained (red colored) by anti-CD34. The tumor vessel densities in both groups of (b) ultrasound (US) alone and (c) TNP-470 treatment alone were significantly lower than that of (a) the control. The reduction of tumor vessel density was significantly enhanced by (d) the combined treatment, in comparison to that of (b) the US treatment alone, or (c) the TNP-470 alone. The destruction of tumor vessels (→) and areas of coagulative necrosis (upper areas in both b and d) are apparently shown in either US treatment alone or after combination treatment. Scale bars: 200 μ m.

using either non-contrasted color Doppler or power Doppler ultrasound because the intensity of the signals of the colored-blood flow in these approaches were apparently lower than that of contrasted color Doppler ultrasound.

MVD. The mean of AIMVD in each treatment group was significantly lower than that of the control (unpaired *t*-test, US: $P = 0.0008$; TNP-470: $P = 0.002$; combination: $P = 0.0001$). The reduction of AIMVD was significantly enhanced by the combined treatment, in comparison to that of the TNP-470 treatment alone ($P = 0.04$). In contrast, no difference in the mean of HIMVD was observed between the group of either US treatment alone or TNP-470 treatment alone and the control ($P = 0.94$, $P = 0.13$). However, the reduction of HIMVD was significantly enhanced by the combined treatment, in comparison to that of the US treatment alone ($P = 0.0001$), or the TNP-470 alone ($P = 0.001$; Table 1; Fig. 5a–d). The destruction of the tumor vessels and areas of coagulative necrosis were apparently seen in tumors of either US therapy alone or combination treatment, in comparison to either the control or TNP-470 treatment alone group.

Toxicity. No side-effect such as a loss of body weight, or neurotoxicity was significantly observed in any mice in this study.

Discussion

TNP-470 blocks endothelial cell cycle progression in the late G1 phase to activate p53 in endothelial cells, thus leading to an increase in cyclin-dependent kinase inhibitor p21^{CIP/WAF} expression and subsequent growth arrest.⁽¹⁰⁾ The molecular target of TNP-470 has been found to be MetAP-2, an intracellular enzyme necessary for the process of protein myristylation, thus preventing membrane proteins from translocating to the cell surface.⁽⁹⁾ Moreover, TNP-470 suppresses the production of bFGF, or VEGF *in vitro*.^(5,13) TNP-470 has been shown to act for human malignancies as a single agent in a wide variety of preclinical models^(11–13) and some clinical trials.^(27,28) Recent studies have showed a synergistic effect of radiation and angiogenesis inhibitors.^(6,7) The combination of angiostatin, an antiangiogenic agent, and radiotherapy has been shown to work best when angiostatin was given simultaneously with radiotherapy *in vivo*.⁽⁶⁾ The successful outcome from the combination of TNP-470 with cytotoxic therapies⁽⁵⁾ or radiotherapy⁽¹⁵⁾ has been also shown *in vivo*.

Weight loss has been frequently observed in animals receiving TNP-470, and the dose-limiting neurotoxicity associated with

TNP-470 has been reported in clinical trials.⁽²⁸⁾ In the present study, the dose of TNP-470 was thus kept low (30 mg/kg/day, three times/week), so that no remarkable side-effects were observed in any mice treated using TNP-470 with or without US irradiation. To reduce the toxicity of TNP-470, however, a recent study tried using water-soluble synthetic polymers, *N*-(2-hydroxypropyl) methacrylamide (HPMA) copolymer, as a specific carrier of TNP-470, so that this HPMA copolymer-TNP-470 substantially enhanced and prolonged the activity of TNP-470 *in vivo* and did not cause any weight loss or neurotoxic effects in mice.⁽²⁹⁾ Further approaches or new ideas may be required to reduce the toxicity of antiangiogenic agents.

US, which is routinely used for diagnostic imaging applications, is now being adopted in various therapeutic applications. The effect of US in activating antitumor drugs or agents has been studied both *in vitro* and *in vivo*.^(16,17,19) Our previous study showed that leukemia cells could be selectively eliminated using low-intensity US in the presence of photosensitive drugs.⁽²²⁾ The mechanism behind the augmentation of the activity of anticancer drugs and other agents by US remains to be fully elucidated; however, several mechanisms have been suggested: i) increased permeability: the increased intracellular concentration of drugs after ultrasonic irradiation suggests an increased permeability (also called sonoporation), or the opening of pores in the cells.⁽²⁰⁾ Sonoporation is the term used for the phenomenon by which US may transiently alter the structure of the cellular membrane, thus inducing an enhanced uptake of low- and high-molecular-weight molecules into the cell. There have been a large number of studies in which a synergistic effect between US and different drugs has been sought. Regarding the mechanisms of action in an *in vitro* environment, acoustic cavitation and streaming may be predominant.⁽³⁰⁾ Our previous study showed that a direct observation of the cells using electron microscopy confirmed the presence of pore-like disruptions in the cell membrane after the combined treatment;⁽²¹⁾ ii) increased sensitivity of the cells to the agent: US alone can cause lethal or sublethal cellular damage.⁽³¹⁾ Interestingly, our current study also showed that US alone could inhibit the growth of a FU-MMT-1 xenograft established from a uterine sarcoma,⁽¹⁴⁾ which is one of the most aggressive tumors among the human malignancies. Moreover, histopathologically, the destruction of tumor vessels and area of coagulative necrosis were apparently seen in tumors treated with either US therapy alone or combination treatment, compared to those treated with

TNP-470 therapy alone, thus suggesting direct cellular damage by US irradiation. One commonly observed vascular effect, usually characterized by an increased tumor blood flow during the initial period of therapeutic US irradiation and eventual destruction of the vasculature, renders the tumor mass more hypoxic.⁽³¹⁾ Our current study supported the vascular effect of US *in vivo* because the mean AIMD in US treatment alone was significantly lower than that of control, and destruction of tumor vessels was apparently seen in the US treatment group. A recent study showed that malignant cells were found to be sensitive to therapeutic US treatment, thus resulting in a transient decrease in cell proliferation.⁽³²⁾ In a suspension of carcinoma cells exposed to 1 MHz ultrasound, cell killing was induced, accompanied by DNA strand breaks. This might be mainly attributable to free radical formation and the pyrolytic processes.⁽²⁴⁾ Cells damaged sublethally by US are thus suggested to be more biologically susceptible to the antitumor agents; iii) potentiation of the agent: it is also suggested that anticancer agents became more potent against tumor cells when they are used in conjunction with US.^(16,17,19) The absorption of US energy by the agent and the production of free radicals have been cited as the likely mechanisms of this increase.⁽³³⁾ Inertial cavitation is required in this process, primarily in the production of free radicals.⁽¹⁸⁾ We thus irradiated with low-intensity US within a few minutes after the subcutaneous injection of TNP-470 to accelerate the drug potentiation because the mean plasma half-life of TNP-470 has been reported to be short (2–6 min in humans by intravenous injection).⁽²⁸⁾ As a result, this combined treatment could significantly inhibit the growth of FU-MMT-1 *in vivo*, in comparison to either TNP-470 used alone or US alone, thus suggesting an accelerated (booster, or synergistic) effect of US for TNP-470. We suppose that the possible mechanism of our combination therapy using a low-intensity US might be chiefly the first mechanism (sonoporation) described above.

As TNP-470 has been shown to possess antiproliferation effects for not only endothelial cells but also for tumor cells, the uptake of this agent might thus be enhanced in both cells by sonoporation. In addition, direct cellular damage including a vascular effect by US irradiation (the second mechanism) might be added because of the evidence of wide areas of coagulative necrosis in irradiated tissue specimens. Feril *et al.* recently reported monocytic leukemia cells (U937) were killed by combining hyperthermia sensitive drug, 2,2'-azobis (2-amidinopropane) dihydrochloride (AAPH) and exposure to non-thermal 1 MHz US for 1 min at an intensity of 2.0 W/cm².⁽³⁴⁾ Apoptosis measured using flow cytometry and free radical investigation using electron paramagnetic resonance (EPR) spin trapping showed that US-induced cell lysis and apoptosis were enhanced in the presence of AAPH, regardless of the temperature at the time of sonication. Although free radicals were increased in the combined treatment, this increase did not correlate well with cell killing.⁽³⁴⁾ The mechanism of enhancement pointed to the increased uptake of the agent during sonication rather than potentiation by AAPH. However, direct measurement of free radicals in the present experiment was technically impossible and further analysis will be needed to affirm these suppositions.

US has been used as a modality for diagnostic imaging in various clinical fields without producing any significant adverse effects. The neovascularization of tumors could be displayed using

color Doppler US in various human solid tumors. The changes in intratumoral vascularity in xenotransplanted tumors treated using antiangiogenesis have been demonstrated using color Doppler US in real-time.^(35,36) In our recent clinical report, using color Doppler US with a microbubble contrast agent was shown to enhance the vascularity of solid tumors, even in small lesions.⁽³⁷⁾ In the present study, the outcome of antiangiogenic treatment thus could be more efficiently evaluated using contrast color Doppler US than non-contrast Doppler. Our histopathological results supported the findings of sonographic vascular density and, immunohistochemically, both HIMVD and AIMVD in the combined treatment group were significantly lower than those in the TNP-470 treatment alone group. The discrepancy in the results between the HIMVD and AIMVD in US treatment alone as well as in TNP-470 treatment alone might be the result of the alternative angiogenesis (increased vascularity) focally seen near the hypoxic areas. In the present study, although a difference in the results of vascular density between color Doppler sonography and immunohistochemical examination was partially observed, another recent study has also showed the usefulness of contrast color Doppler to assess angiogenesis without an immunohistochemical examination *in vivo*.⁽³⁵⁾ Moreover, another study additionally reported that the color Doppler vascularity index is a better indicator of tumor behavior than the immunohistochemical microvessel density in colon cancer patients.⁽³⁸⁾ As a result, the combined treatment of TNP-470 and US irradiation was found to be more effective in suppressing angiogenesis for uterine sarcoma xenografts than either therapy alone. The mechanisms of this antiangiogenic therapy using low-intensity US for intratumoral microvessels as well as feeding vessels into the tumors therefore need to be more precisely elucidated.

The xenotransplanted model used in this study is originated from a human uterine carcinosarcoma,⁽¹⁴⁾ which is one of the highest angiogenic tumors in all human solid malignancies. Our previous studies apparently showed higher expressions of VEGF-A and angiopoietin-2 genes as well as a higher frequency of lymphovascular invasion and a high-MVD of these tumors, in comparison to those of the other human uterine carcinomas.^(26,39) As a result, the success of the antiangiogenic combination therapy used in the present study might therefore be associated with the high angiogenic activities (vascular-rich) of this tumor. Further trials of this combination therapy for other tumor models with either moderate or low levels of angiogenic activity might therefore be needed.

In conclusion, our results support the positive interaction between TNP-470 and US energy regarding the inhibition of growth, and angiogenesis of human uterine sarcoma. As a result, US irradiation is thus suggested to have enhanced the effect in antiangiogenesis therapy on this tumor, and this combination might be potentially useful for a new cancer therapy.

Acknowledgments

This research was partly supported by a grant from the Ministry of Education, Science and Culture, Japan (#11671164). A part of the content in this study was orally announced by the first author as the 'Effect of antiangiogenesis drug therapy combined with ultrasound irradiation for uterine cancer evaluated with contrasted ultrasonography' at the 14th World Congress on Ultrasound in Obstetrics and Gynecology at Stockholm, Sweden, September 4, 2004.

References

- 1 Folkman J. Tumor angiogenesis: Therapeutic implications. *N Engl J Med* 1971; 285: 1182–6.
- 2 Carmeliet P, Jain RK. Angiogenesis in cancer and other diseases. *Nature* 2000; 407: 249–57.
- 3 Willett CG, Boucher Y, di Tomaso E *et al.* Direct evidence that the VEGF-specific antibody bevacizumab has antivascular effects in human rectal cancer. *Nat Med* 2004; 10: 145–7.
- 4 Herbst RS, Madden TL, Tran HT *et al.* Safety and pharmacokinetic effects of TNP-470, an angiogenesis inhibitor, combined with paclitaxel in patients with solid tumors: evidence for activity in non-small-cell lung cancer. *J Clin Oncol* 2002; 20: 4440–7.
- 5 Inoue K, Chikazawa M, Fukata S, Yoshikawa C, Shuin T. Docetaxel enhances the therapeutic effect of the angiogenesis inhibitor TNP-470 (AGM-1470) in metastatic human transitional cell carcinoma. *Clin Cancer Res*, 2003; 9: 886–99.
- 6 Gorski DH, Mauceri HJ, Salloum RM *et al.* Potentiation of the antitumor